Syst. Biol. 65(2):304–327, 2016

DOI:10.1093/sysbio/syv088
Advance Access publication November 24, 2015

Cryptic Species or Inadequate Taxonomy? Implementation of 2D Geometric Morphometrics Based on Integumental Organs as Landmarks for Delimitation and Description of Copepod Taxa

TOMISLAV KARANOVIC[1,2,*], MARKO DJURAKIC[3], AND STEFAN M. EBERHARD[4,5]

[1]*Department of Biological Science, College of Science, Sungkyunkwan University, Suwon 440-746, Korea;* [2]*Institute for Marine and Antarctic Studies, University of Tasmania, Hobart, Tasmania 7001, Australia;* [3]*Department of Biology and Ecology, Faculty of Science, University of Novi Sad, Trg Dositeja Obradovića 2, Novi Sad 21000, Serbia;* [4]*Subterranean Ecology Pty Ltd, Coningham, Tasmania 7054, Australia; and* [5]*Connected Waters Initiative Research Centre, University of New South Wales, Sydney 2052, Australia*

[*]*Correspondence to be sent to: Department of Biological Science, College of Science, Sungkyunkwan University, Suwon 440-746, Korea; E-mail: Tomislav.Karanovic@utas.edu.au.*

Tomislav Karanovic and Marko Djurakic contributed equally to this article.

Received 25 June 2015; reviews returned 13 November 2015; accepted 13 November 2015
Associate Editor: Frank Anderson

Abstract.—Discovery of cryptic species using molecular tools has become common in many animal groups but it is rarely accompanied by morphological revision, creating ongoing problems in taxonomy and conservation. In copepods, cryptic species have been discovered in most groups where fast-evolving molecular markers were employed. In this study at Yeelirrie in Western Australia we investigate a subterranean species complex belonging to the harpacticoid genus *Schizopera* Sars, 1905, using both the barcoding mitochondrial COI gene and landmark-based two-dimensional geometric morphometrics. Integumental organs (sensilla and pores) are used as landmarks for the first time in any crustacean group. Complete congruence between DNA-based species delimitation and relative position of integumental organs in two independent morphological structures suggests the existence of three distinct evolutionary units. We describe two of them as new species, employing a condensed taxonomic format appropriate for cryptic species. We argue that many supposedly cryptic species might not be cryptic if researchers focus on analyzing morphological structures with multivariate tools that explicitly take into account geometry of the phenotype. A perceived supremacy of molecular methods in detecting cryptic species is in our view a consequence of disparity of investment and unexploited recent advancements in morphometrics among taxonomists. Our study shows that morphometric data alone could be used to find diagnostic morphological traits and gives hope to anyone studying small animals with a hard integument or shell, especially opening the door to assessing fossil diversity and rich museum collections. We expect that simultaneous use of molecular tools with geometry-oriented morphometrics may yield faster formal description of species. Decrypted species in this study are a good example for urgency of formal descriptions, as they display short-range endemism in small groundwater calcrete aquifers in a paleochannel, where their conservation may be threatened by proposed mining. [Barcoding; cuticular pore; integrative taxonomy; sensillum; speciation; stygofauna.]

Estimation and characterization of species diversity is important from both fundamental and applied perspectives. As "species" is the operational unit for biodiversity, defining species boundaries represents the mainstay for biodiversity quantification and management, and its conceptualization has received a considerable intellectual effort (Sites and Marshall 2003; de Queiroz 2007). Species delimitation is traditionally assessed by comparing variability in organisms' morphological traits, and in some cases physiological, developmental, behavioral, and ecological traits, and also, increasingly, genetic traits (Padial et al. 2010). Frequently, however, evolutionary history (e.g., pattern and rate) of compared traits differs within a particular lineage, which in turn impedes species delimitation. The failure to detect so-called "cryptic" or "hidden" species results in underestimation of true levels of biodiversity (Lefébure et al. 2006; Padial et al. 2010; Vodă et al. 2014) and it is now well established that cryptic species occur in most animal groups (Bickford et al. 2007; Pfenninger and Schwenk 2007). "Cryptic" species refers to two or more species that were not distinguished morphologically at the time of original description and are erroneously classified under the same scientific name. Many cryptic species are detected by subsequent molecular analysis, sometimes many years later, so emergence of "integrative taxonomy" as a discipline brings an operational framework that evaluates several lines of evidence in order to delimit species boundaries (Dayrat 2005; Pante et al. 2015). Even when several lines of evidence consistently disagree and therefore impede species delimitation for a considerable time, the utility of integrative taxonomy, combined with evolutionary explanations, advances knowledge of species boundaries and evolutionary processes simultaneously and provides solid nomenclatural outcomes (Andújar et al. 2014).

Taxonomy studies today are strongly biased toward vertebrates (Gaston and May 1992; Pante et al. 2015), even though they account for only approximately 3% of the described species diversity on Earth (Zhang 2011). Copepods and other aquatic arthropods unquestionably deserve more research effort. Even though cryptic species occur in most animal groups, it is clear that groups with well-studied morphology and specimens of large size show this phenomenon much less. For example, after barcoding 260 North American bird species Hebert et al. (2004) discovered only four possible cryptic species. In contrast, in subterranean faunas numerous cryptic species may be revealed by molecular

analysis owing to the typically conservative and convergent morphology resulting from evolutionary troglogenesis (Guzik et al. 2011). In Western Australia for example, numerous cryptic species of amphipod crustaceans have been revealed initially by molecular analysis (Finston et al. 2007; Bradford et al. 2010), which has triggered closer scrutiny and subsequent detection of morphological differences (King et al. 2012). As copepods are smaller and therefore more difficult to study than amphipods, it comes as no surprise that studies of some fast-evolving mitochondrial markers suggested several morphospecies to actually be complexes of cryptic species (Bláha et al. 2010; Hamrova et al. 2012). Karanovic and Krajicek (2012a) proposed previously understudied microstructures, such as integumental organs, as a useful tool to distinguish newly discovered cryptic species. However, sometimes even detailed non-multivariate studies of these microstructures failed to provide morphological characters for delimitation of cryptic species detected using molecular tools (Karanovic and Cooper 2012).

All arthropods have their bodies covered by a rigid cuticle, which protects their inner organs and tissues but at the same time impedes communication with the surrounding environment. A significant proportion of this communication is thus achieved through sensilla and pores, small cuticular organs which cover vast areas of their body (Hallberg and Hannson 1999). Their very different size, structure, number, and function suggest that it would be difficult to homologize them in different arthropod groups (Crouau 1997; Keil 1997; Hallberg and Skog 2011), although some researchers have implied homology through common or analogous terminologies for insect and crustacean cuticular organs (Shelton and Laverack 1968; Fleminger 1973). Even within crustaceans their diversity is astonishing. A quick look through several complete or partial surveys of cuticular organs in some groups of decapods (Mauchline 1977), amphipods (Oshel et al. 1988; Zimmer et al. 2009), isopods (Powell and Halcrow 1982; Khalaji-Pirbalouty 2014), branchiopods (Cash-Clark and Martin 1994; Boundrias and Pires 2002), cephalocaridans (Elofsson and Hessler 1994), ostracods (Puri 1974; Meisch and Wouters 2004), and copepods (Von Vaupel Klein 1982a) reveals a plethora of specialized sensilla and pores (and their terminology), some of which hold a potential to increase the number of recognized synapomorphies for certain taxa. Diversity of cuticular organs reported for copepods alone comprises at least some 20 distinct types (Von Vaupel Klein 1982a). Despite the fact that many studies have advocated the phylogenetic potential of these characters, and proposed some groupings based on intuitive methods (Puri 1974; Mauchline 1988; Tsukagoshi 1990; Olesen 1996; Høeg and Kolbasov 2002), the first study that tested their phylogenetic value in any group of crustaceans was not done until very recently (Karanovic and Kim 2014a). This is in stark contrast with taxonomic and phylogenetic practices in some other groups of small animals with a rigid integument, such as, for example, insects (Alarie 1998; D'Haese 2003; Faucheux et al. 2006), mites (Shen et al. 2014), tardigrades (Nichols et al. 2006), and kinorhynchs (Nebelsick 1992; Sørensen et al. 2012).

Employing molecular techniques was one of the priorities of our study to aid in species delimitation and reconstruction of their phylogenetic relationships. DNA-based species identification methods, referred to as "DNA barcoding", have been widely employed to estimate levels of species diversity, with the 5′-end of the mitochondrial COI gene proposed as the "barcode" for all animal species (Hebert et al. 2003). The advantage of the mtCOI gene is that it often shows low levels of genetic variation within species, but high levels of divergence between species; for the most common divergence values in a variety of crustacean taxa see Lefébure et al. (2006) and for harpacticoid copepods see Karanovic and Cooper (2011a, 2011b, 2012) and Karanovic and Kim (2014b). In recent years several studies on copepods showed that combining molecular and morphological methods can help answer questions related to cryptic speciation (Bláha et al. 2010; Hamrova et al. 2012), invasions of new habitats and colonization pathways (Lee et al. 2003; Winkler et al. 2008; Karanovic and Cooper 2011a, 2012), anthropogenic translocation (Karanovic and Krajicek 2012a), short-range endemism (Karanovic and Cooper 2011a), suitability of novel micromorphological characters (Karanovic and Kim 2014a), and definition of supraspecific taxa in conservative genera or families (Huys et al. 2006, 2012; Karanovic and Cooper 2011b; Karanovic and Krajicek 2012b).

There is no question that a combined morphological and molecular approach results in a much more thorough study (Will et al. 2005; Padial et al. 2010), but most research detecting cryptic speciation does not lead to species descriptions (Pante et al. 2015). This may inflate alpha diversity estimation and in some cases pose an important economic impact (Chessman et al. 2007; Morrison et al. 2009). In this article we aim to follow through with description of the new taxa resulting from our analyses, consistent with sound taxonomic practice that satisfies the International Commission on Zoological Nomenclature (ICZN) (1999). As advocated by many researchers, not linking biological data to a formal species name results in these data losing tremendous value (Goldstein and DeSalle 2011; Platnick 2013), and taxa have to be named to benefit from any conservation program (Mace 2004; Karanovic et al. 2013b). Established lists of species names represent starting points for a majority of research programs, natural resource management, and biodiversity conservation (Costello et al. 2013; De Carvalho et al. 2014).

In the present article we tackle the *Schizopera akation* Karanovic and Cooper, 2012 species-complex from the Yeelirrie paleochannel in Western Australia, using two-dimensional (2D) geometric morphometrics based on integumental organs as landmarks. We believe this is the first time this approach has been tried in any crustacean group. We aim to test if the mtCOI gene is more sensitive than the 2D geometric morphometrics.

In this way we compare two different methods for species delimitation, consistent with emerging trends in systematic biology (Marshall et al. 2006; Pons et al. 2006; Wiens 2007; Carstens et al. 2013). Landmark-based geometric morphometrics has been employed to solve a variety of questions from the broader context of ecology and evolution (Collyer and Adams 2013), evolutionary developmental biology (Parsons and Albertson 2013; Sanger et al. 2013), and biogeography (Meloro et al. 2013, 2014). Coupled with high statistical power, this method is suitable for detecting even subtle variation, such as asymmetry of morphological structures (Klingenberg and McIntyre 1998; Klingenberg et al. 2002). A quantification and discrimination of variation that is not visible by the human eye makes geometric morphometrics a valuable tool for detecting cryptic species (Adams and Funk 1997; Baylac et al. 2003; Milankov et al. 2009; Francuski et al. 2011; Yu et al. 2013; Barão et al. 2014; Mitrovski-Bogdanović et al. 2014; Schwarzfeld and Sperling 2014). To provide a broader perspective for our comparison, we examine molecular phylogeny of the *S. akation* complex and chosen landmark sensilla and pores in a wider group of congeners.

Materials and Methods

Specimen Collection

In total, 119 specimens belonging to 11 morphospecies were used for our survey of selected integumental organs (Figs. 1 and 2) using scanning electron microscopy (SEM) (Table 1), while 49 specimens of *S. akation* were sampled for morphometric analyses (Table 2). An additional 39 *Schizopera* Sars, 1905 specimens, belonging to 12 morphospecies, as well as four *Stenhelia* Boeck, 1865 specimens, belonging to two morphospecies, were used for our molecular analyses (Table 1). The holotype of *S. akation* was not used in this study, as it was dissected and mounted in a permanent medium (see Karanovic and Cooper 2012), but all specimens belonging to our Clade A are topotypes.

Most samples of *Schizopera* studied here were collected in shallow groundwater calcrete aquifers on Yeelirrie Station (Fig. 3) in the Yilgarn region of Western Australia (see Karanovic and Cooper 2012). Two other *Schizopera* species were collected from groundwaters in the Pilbara region of Western Australia (see Karanovic and McRae 2013). One species was collected from Japan, in subterranean waters in the vicinity of the ancient Lake Biwa (see Karanovic et al. 2015). Two species of the marine genus *Stenhelia* were collected from shallow littoral habitats in Korea and Russia (see Karanovic et al. 2014) and used as outgroups for our molecular analyses, as well as for rooting the trees. The latter belong to the same family as *Schizopera* (Miraciidae), but to a different subfamily (Stenheliinae) (see Karanovic and Kim 2014b). All Australian specimens are deposited in the Western Australian Museum (WAM), Perth, Western Australia; the Japanese specimens are deposited in the Lake Biwa Museum (LBM), Kusatsu, Shiga prefecture; and the specimens belonging to our two outgroup taxa are deposited in the National Institute of Biological Resources (NIBR), Incheon, South Korea.

Samples from Australia were collected with haul nets from groundwater bores of various salinity (Karanovic and Cooper 2012); those from Japan were collected from freshwater hyporheic habitats using Bou-Rouch style phreatic samplers, similar to those used by Tanaka et al. (2014); the Korean outgroup was collected from muddy sediments with a Van Veen grab sampler (Karanovic et al. 2014), then subsamples were taken using acrylic corers and animals were extracted using Ludox method (Burgess 2001); the Russian outgroup was collected with a hand-net from a sandy bottom using SCUBA (Karanovic et al. 2014). Samples were preserved in the field in cold 99.9% ethanol, kept on ice or in a refrigerator, and sorted in a laboratory. Specimens for SEM were dehydrated in progressive ethanol concentrations, transferred into pure isoamyl-acetate, critical-point dried, mounted on stubs, coated in gold, and observed under a Hitachi S-4700 microscope on the in-lens detector, with an accelerating voltage of 10 kV and working distances between 12.3 and 13.4 mm.

Molecular Data Collection

Specimens for molecular analyses were examined without dissecting under a Leica MB2500 phase-interference compound microscope (objective 63 × dry) in propylene glycol. After examination they were returned to 100% ethanol. DNA from Australian specimens was extracted using the GENTRA method (Puregene) according to the manufacturer's protocol for fresh tissues. PCR amplifications of a 623-bp fragment from the mitochondrial COI gene were carried out with the "universal" primers LCOI490 and HCO2198 (Folmer et al. 1994). When needed, additional "nested" primers, designed by Ms Kathleen Saint (South Australian Museum) from preliminary copepod COI sequence data, were used in combination with the universal primers to improve the PCR amplification efficiency (Karanovic and Cooper 2012). An initial PCR amplification used the combination LCOI490/HCO2198, and then 1 μμL of product was used to seed nested PCRs in the following combinations: M1323/HCO2198 or M1321/M1322. PCR amplifications were carried out in 25 μL volumes containing: 4 mM $MgCl_2$, 0.20 mm dNTPs, 1 × PCR buffer (Applied Biosystems), 6 pmol of each primer, and 0.5 U of AmpliTaq Gold (Applied Biosystems). PCR amplification was performed under the following conditions: initialization at 94°C for 9 min; then 34 cycles of denaturation at 94°C for 45 s, annealing at 48°C for 45 s, elongation at 72°C for 60 s, with a final elongation step at 72°C for 6 min. PCR products were purified using a vacuum plate method and sequencing was undertaken using the ABI prism Big Dye Terminator Cycle sequencing kit

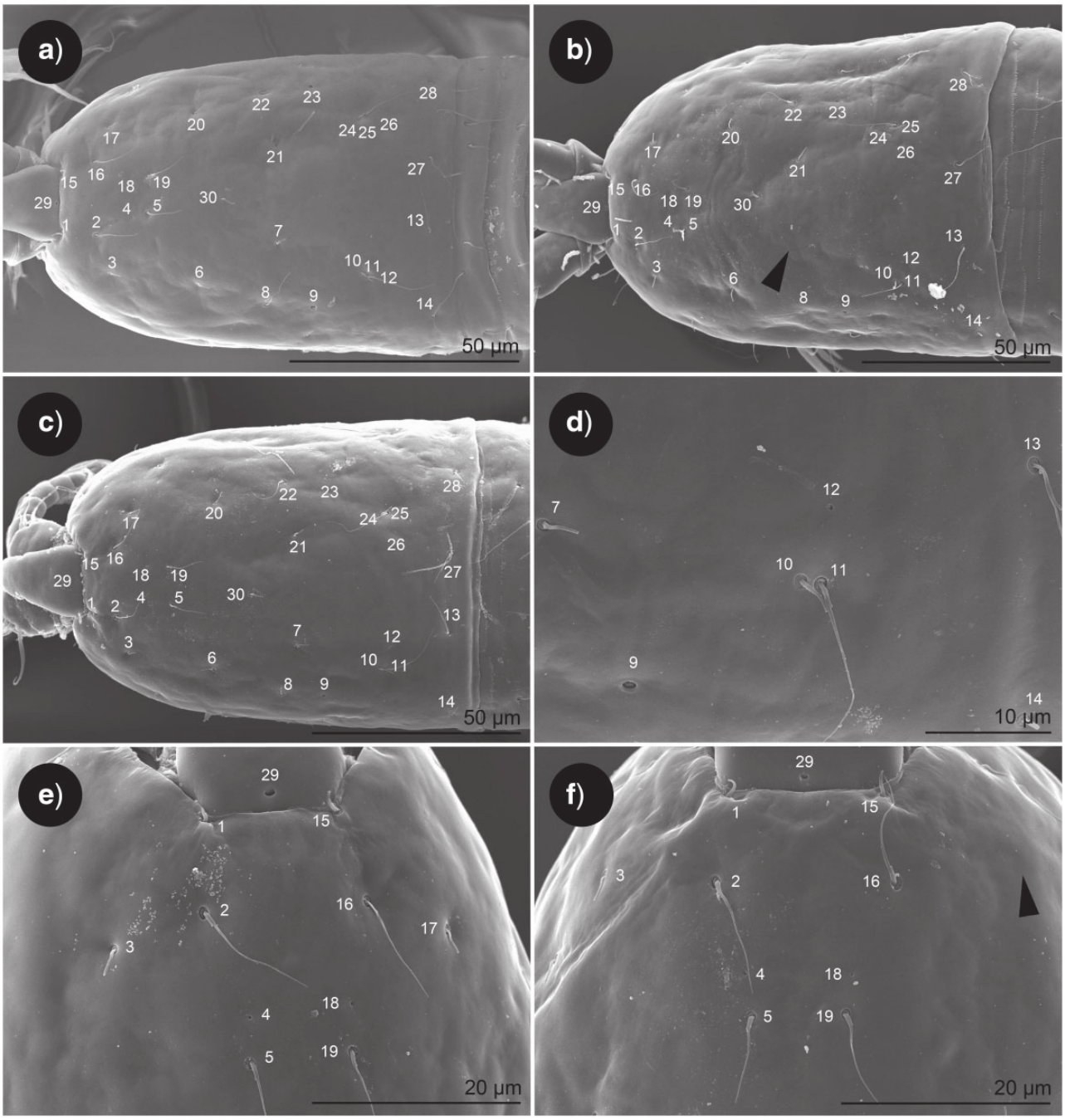

FIGURE 1. Landmark (LM) sensilla and pores on the cephalothorax in six specimens of *Schizopera akation* Karanovic and Cooper, 2012, belonging to three different molecular clades (see Figs. 3 and 4): a) female 1 from bore SB14-1 (clade A); b) female from bore YYD22 (clade C); c) female 1 from bore L-UNK1 (clade B); d) female 2 from bore L-UNK1 (clade B); e) male from bore L-UNK1 (clade B); f) female 2 from bore SB14-1 (clade A). Arrowheads mark absent LMs 7 and 17 in b and f, respectively.

(PE Applied Biosystems, Foster City, CA) on an ABI 3700 DNA analyser (Applied Biosystems). DNA from Korean, Russian, and Japanese specimens was extracted using the LaboPassTM extraction kit (COSMO Co. Ltd, Korea) and following the manufacturer's protocols for fresh tissue, except that samples were incubated in the Proteinase K solution overnight, Step 5 was skipped, and 60 instead of 200 µµL of Buffer AE was added in the final step, to increase the density of DNA. Amplifications were made using PCR premix (BiONEER Co.) in TaKaRa PCR thermal cycler (Takara Bio Inc., Otsu, Shiga, Japan), with the following protocol: initial denaturation at 94°C for 300 s; 40 cycles of denaturation at 94°C for 30 s, annealing at 42°C for 120 s, extension at 72°C for 60 s, and final extension at 72°C for 600 s. PCR results were checked by electrophoresis of the amplification

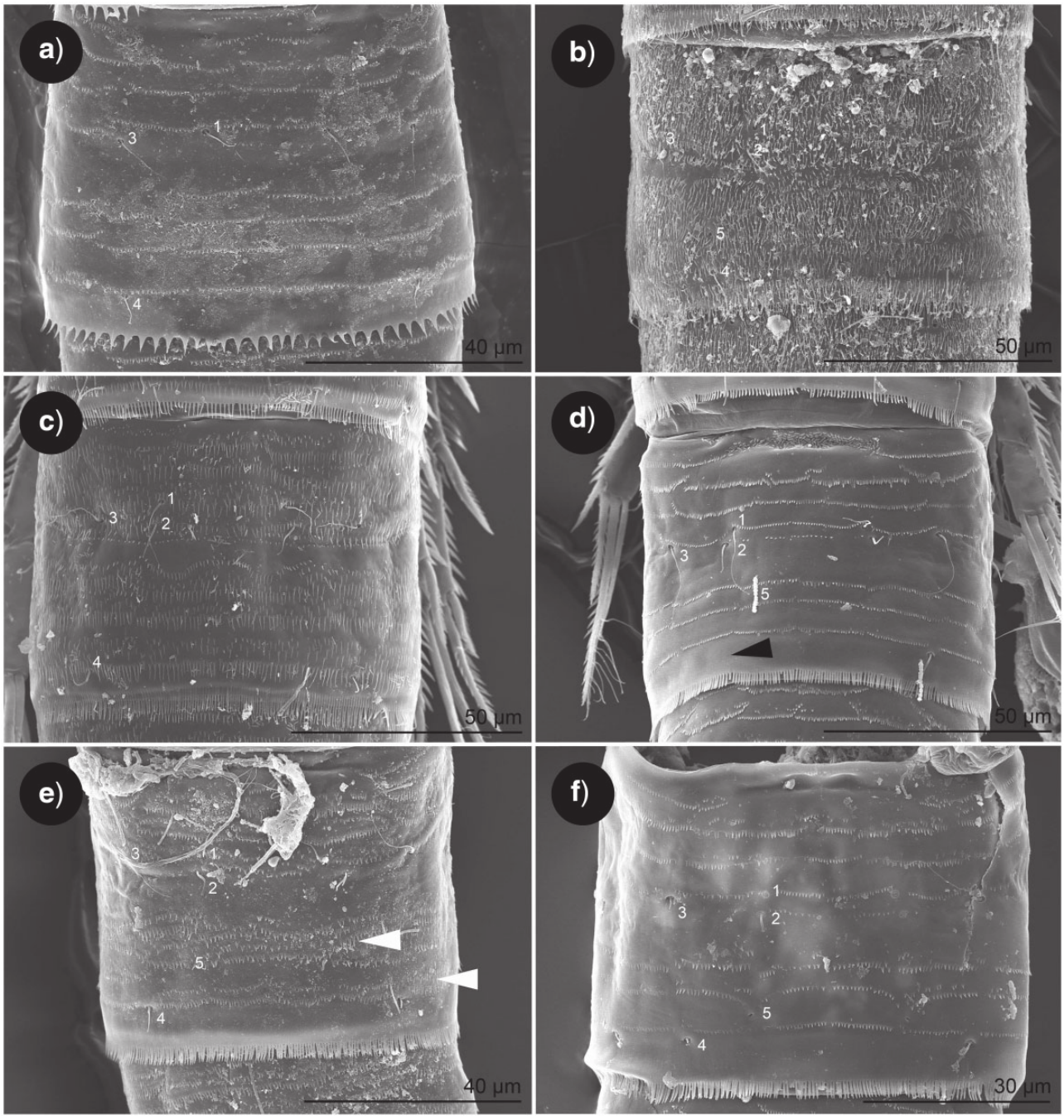

FIGURE 2. Female genital double-somite of four *Schizopera* Sars, 1905 species: a) *S. cooperi* Karanovic and McRae, 2013; b) *S. uranusi* Karanovic and Cooper, 2012; c) *S. analspinulosa analspinulosa* Karanovic and Cooper, 2012; d) *S. akation* Karanovic and Cooper, 2012 from bore YYD22 (clade C); e) *S. akation* from bore SB14-1 (clade A); f) *S. akation* from bore L-UNK1 (clade B; see Figs. 3 and 4). Arabic numerals indicating four sensilla and single pore selected as LMs for *S. akation*. Black arrowhead marks an absent LM 4; white arrowheads mark additional rows of minute spinules.

products on 1% agarose gel with ethidium bromide. PCR products were purified with a LaboPassTM PCR purification kit and sequenced in both directions using a 3730xl DNA analyzer (Macrogen, Korea). The complete mitochondrial genome of *S. knabei* was downloaded from GenBank (see Easton et al. 2014) and trimmed for the largest overlapping range with any other congener after alignment (640 bases), while all other sequences were used with their original lengths, ranging from 407 to 639 bases.

Molecular Data Analysis

Obtained sequences were checked manually and aligned by the ClustalW algorithm (Thompson et al.

TABLE 1. List of species examined for mtCOI DNA and survey of cuticular organs using scanning electron microscope (SEM)

Species	Country	Region	GenBank[a,b]	SEM	Voucher[b]
Schizopera abei Karanovic et al. (2015)	Japan	Shiga	KP867870, 871, 872	10 ♂ + 11 ♀	LBM1430005773
Schizopera akation Karanovic and Cooper (2012)	Australia	Yilgarn	JQ390560, 583, 585, 587, 589	11 ♂ + 13 ♀	WAMC37482, 55908, 55909, 55910
Schizopera akolos Karanovic and Cooper (2012)	Australia	Yilgarn	JQ390584	—	—
Schizopera a. analspinulosa Karanovic and Cooper (2012)	Australia	Yilgarn	JQ390586	5♂ + 7 ♀	WAMC37483, 55911
Schizopera analspinulosa linel Karanovic and Cooper (2012)	Australia	Yilgarn	JQ390563, 588	3 ♂ + 2 ♀	WAMC37477
Schizopera cf. *uranusi* sp. 2	Australia	Yilgarn	JQ390571	—	—
Schizopera cooperi Karanovic and McRae (2013)	Australia	Pilbara	JQ390555	4 ♂ + 3 ♀	WAMC47246
Schizopera emphysema Karanovic and Cooper, 2012	Australia	Yilgarn	JQ390558	2 ♂	WAMC55912
Schizopera knabei Lang, 1965	USA	Unknown	KF667527	—	—
Schizopera kronosi Karanovic and Cooper (2012)	Australia	Yilgarn	JQ390559, 567, 756	5♂ + 2 ♀	WAMC55913
Schizopera leptafurca Karanovic and Cooper (2012)	Australia	Yilgarn	JQ390557, 565, 566, 568, 569, 570, 574, 575, 578, 580, 582, 590	4 ♂ + 5 ♀	WAMC37490, 55914
Schizopera sp. 2	Australia	Pilbara	JQ390556, 572	—	—
Schizopera uranusi Karanovic and Cooper (2012)	Australia	Yilgarn	JQ390561, 562, 564, 573, 577, 579, 581	15 ♂ + 8 ♀	WAMC37494, 55915
Stenhelia pubescens Chislenko, 1978	Russia	Far East	KF524870, 871	2 ♀	NIBRIV0000232715
Stenhelia taiae Mu and Huys, 2002	Korea	South Sea	KF524884, 885	2 ♂ + 5 ♀	NIBRIV0000232718, 287229

[a]Each GenBank accession number represents one separate specimen and for their precise locality data see Karanovic and Cooper (2012), Karanovic and McRae (2013), Karanovic et al. (2014, 2015), and Easton et al. (2014).
[b]Subsequent GenBank numbers and voucher codes for specimens on separate SEM stubs are abbreviated in each cell.

TABLE 2. List of *Schizopera akation* specimens sampled for 2D geometric morphometrics

Clade[a]	Calcrete[b]	Line[c]	Locality[d]	Date	Code[e]	Sex	Cth[f]	GS[g]
A	SB14	SB14	SB14-1	11-iii-2009	LN6492f1	♀	+	+
A	SB14	SB14	SB14-1	21-ix-2010	10:0535ef1	♀	+	+
A	SB14	SB14	SB14-1	21-ix-2010	10:0535ef2	♀	+	+
A	SB14	SB14	SB14-1	18-iii-2010	LN8182f1	♀	+	+
A	SB14	SB14	SB14-1	18-iii-2010	LN8182m1	♂	+	−
A	SB14	SB14	SB14-1	18-iii-2010	LN8182m2	♂	+	−
A	SB14	SB14	SB14-1	18-iii-2010	LN8182m3	♂	+	−
A	SB14	SB14	SB14-1	21-ix-2010	10:0535em1	♂	+	−
A	SB14	SB14	SB14-1	21-ix-2010	10:0535em2	♂	+	−
B	L	Line L	L-UNK1	12-x-2010	LN7360f1	♀	+	+[h]
B	L	Line L	L-UNK1	18-iii-2010	LN7139f1	♀	+	+
B	L	Line L	L-UNK1	18-iii-2010	LN7139f2	♀	+	+
B	L	Line L	L-UNK1	16-iii-2010	LN8533f1	♀	+	+
B	L	Line L	L-UNK1	16-iii-2010	LN8533f2	♀	+	+
B	L	Line L	L-UNK1	16-iii-2010	LN8533f3	♀	+	+
B	L	Line L	L-UNK1	16-iii-2010	LN8533f4	♀	+	+
B	L	Line L	L-UNK1	18-iii-2010	LN7139m1	♂	+	−
B	L	Line L	L-UNK1	18-iii-2010	LN7139m2	♂	+	−
B	L	Line L	L-UNK1	18-iii-2010	LN7139m3	♂	+	−
B	L	Line L	L-UNK1	16-iii-2010	LN8533m1	♂	+	−
B	L	Line L	L-UNK1	16-iii-2010	LN8533m2	♂	+	−
B	L	Line L	YYHC0050B	23-iii-2010	LN9980cm1	♂	+	−
B	L	Line L	YYHC0050B	23-ix-2010	LN9980cm2	♂	+	−
C	Yeelirrie	Line 1	YYAC0018C	16-iii-2010	LN8355m1	♂	+	−
C	Yeelirrie	Line 1	YYD22	15-iii-2010	LN8496f1	♀	+	+
C	Yeelirrie	Line 1	YYD22	15-iii-2010	LN8496f2	♀	+	+
C	Yeelirrie	Line 1	YYD22	15-iii-2010	LN8496f3	♀	+	+
C	Yeelirrie	Line 1	YYD22	15-iii-2010	LN8496f4	♀	+	+
C	Yeelirrie	Line 1	YYD22	15-iii-2010	LN8496f5	♀	+	+
C	Yeelirrie	Line 1	YYD22	15-iii-2010	LN8496f6	♀	+	+
C	Yeelirrie	Line 1	YYD22	15-iii-2010	LN8496f7	♀	+	+
C	Yeelirrie	Line 1	YYD22	15-iii-2010	LN8496f8	♀	+	+
C	Yeelirrie	Line 1	YYD22	15-iii-2010	LN8496m1	♂	+	−
C	Yeelirrie	Line 1	YYD22	15-iii-2010	LN8496m2	♂	+	−
C	Yeelirrie	Line 1	YYD22	15-iii-2010	LN8496m3	♂	+	−
C	Yeelirrie	Line 1	YYD22	15-iii-2010	LN8496m4	♂	+	−
C	Yeelirrie	Line 1	YYD22	15-iii-2010	LN8496m5	♂	+	−
C	Yeelirrie	Line 1	YYD26	20-iii-2010	LN8297f1	♀	+	+
C	Yeelirrie	Line 1	YYD26	20-iii-2010	LN8297f2	♀	+	+
C	Yeelirrie	Line 1	YYD26	15-iii-2010	LN8479f1	♀	+	+
C	Yeelirrie	Line 1	YYD26	15-iii-2010	LN8479f2	♀	+	+
C	Yeelirrie	Line 1	YYD26	15-iii-2010	LN8479f3	♀	+	+
C	Yeelirrie	Line 1	YYD26	20-iii-2010	LN8297m1	♂	+	−
C	Yeelirrie	Line 1	YYD26	20-iii-2010	LN8297m2	♂	+	−
C	Yeelirrie	Line 2	YYAC1004C	21-iii-2010	LN8555f1	♀	+	+
C	Yeelirrie	Line 3	YYAC118	12-xi-2009	LN7389f1	♀	+	−
C	Yeelirrie	Line F	YU1	15-iii-2010	LN8492f1	♀	+	+
C	Yeelirrie	Line F	YU1	15-iii-2010	LN8492m1	♂	+	−
C	Yeelirrie	Line F	YU1	15-iii-2010	LN8492m2	♂	+	−
	Total						49	27

[a]One of three cryptic species detected with molecular markers (see Fig. 4).
[b]One of three disjunct subterranean islands in Yeelirrie where this complex was recorded (see Fig. 3).
[c]Transverse series of bores used both for geological exploration of uranium ore and stygofauna sampling.
[d]Code used for individual sampling bore.
[e]Unique number given to each specimen, based on the unique number given to each sample in the field (see Karanovic and Cooper 2012).
[f]Landmarks acquired on the cephalothorax.
[g]Landmarks acquired on the genital double-somite.
[h]Set of landmarks excluded from our analyses.

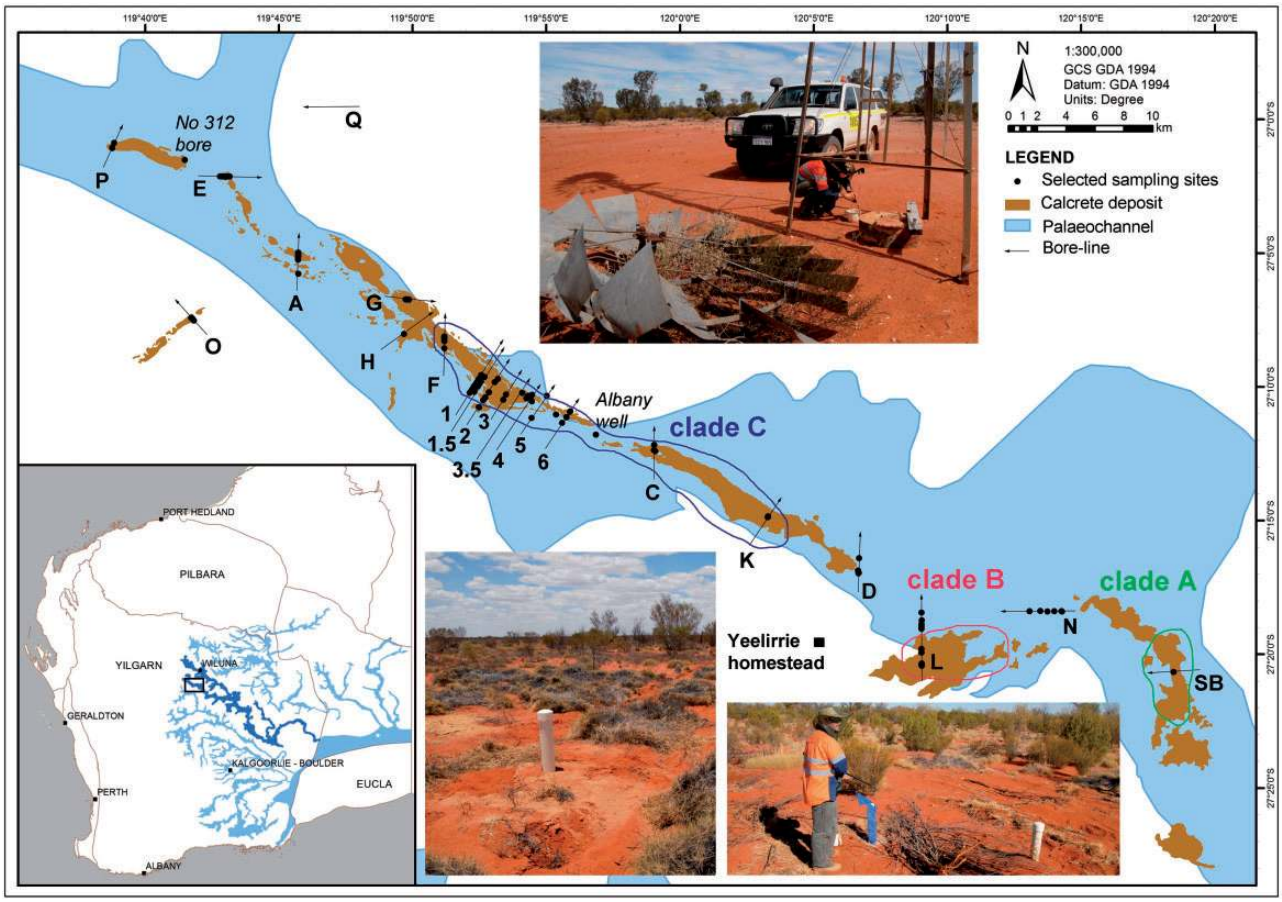

FIGURE 3. Map of the study area showing location of 22 bore-lines, with selection of photographs from sampling localities (bores and wells). The inset shows the locations of the study area in Western Australia. The general subterranean water flow in the paleochannel is from north-west to south-east. Approximate distributions of the three clades of *Schizopera akation* Karanovic and Cooper, 2012, detected with molecular markers (see Fig. 4) are marked as clades A, B, and C and the same letters for them are used throughout this article.

1994) in MEGA 6 (Tamura et al. 2013). The alignment was checked again to make sure that all sites are unambiguously aligned. All sequences were translated into protein using MEGA to check for stop codons, ambiguities, or insertions/deletions indicative of non-functional copies of COI. BLAST analyses of GenBank were used to confirm that the obtained sequences are copepod in origin and not contaminants. The best evolutionary model of nucleotide substitution for our data set was established by the Akaike Information Criterion, performed with jModelTest (Posada and Crandall 1998; Guindon and Gascuel 2003). For the maximum-likelihood (ML) analysis the Hasegawa–Kishino–Yano model (Hasegawa et al. 1985) with gamma distributed rates with invariant sites (HKY+G+I) was selected. Most phylogenetic analyses were conducted using PAUP* 4.0a 144 (Swofford 2003). Maximum parsimony (MP) analysis was conducted using a heuristic search option and the following parameters: TBR branch swapping algorithm, AccTran optimization, "3+1" test, treat gaps as missing data, collapse branches if maximum length is zero, and other default PAUP* settings. ML analysis was conducted using the HKY+G+I model and PAUP* default settings. One thousand bootstrap replicates were performed to obtain a relative measure of node support for the resulting trees. ML pairwise distances (HKY+G+I model) were also computed in PAUP*. For molecular species delimitation we used the Automatic Barcode Gap Discovery (ABGD) web interface (Puillandre et al. 2012), with ML pairwise distances generated in PAUP* as the primary input and the value of the proxy for the minimum gap width (*X*) set to 1.1. We also used the bPTP web interface (Zhang et al. 2013) for molecular species delimitation, using a tree generated with PhyML 3.0 tree (Guindon et al. 2010) under default setting on our original alignment, as the only input. PhyloMap-PTP (Zhang et al. 2011) was used for visualization of the bPTP species delimitation results.

Morphometric Data Collection

Specimens of *S. akation* for morphometric data collection (Table 2) were dissected in half (prosome was separated from urosome) and temporarily mounted on microscope slides in glycerol, with two human

hairs of appropriate thickness mounted between the slide and coverslip. An animals' dorsal perspective that ensures a perpendicular angle to the microscope objective was obtained by manipulating the coverslip carefully by hand, and by checking that symmetrical structures (dorsal pairs of sensilla and pores) were in focus at the same time. Once the specimens were appropriately positioned, pores and sensilla were mapped on a paper using a drawing tube attached to a Leica MB2500 phase-interference compound microscope, always under the same magnification (PL FLUOTAR 100× oil-immersion objective). We selected 30 of them from the cephalothorax (Fig. 1a–c) for all specimens, and 5 from the genital double-somite (Fig. 2f) for females only. To avoid distortion, specimens were consistently oriented under 100× objective and centered with an eyepiece grid. Even though specimens slightly differed in length, their thickness was quite consistent (and well matched with chosen hairs), and distortion due to compression was non-existent.

All selected integumental organs used for geometric morphometric assessment are landmarks (LMs) of type I (Bookstein 1991). Cephalothorax and genital double-somite were mapped independently and analyzed as independent data sets. Of the 30 selected LMs on the cephalothorax only 7 were pores, which included one large medial pore at the base of rostrum (LM 29; see Fig. 1e), one pair of small anterior dorsal pores (LMs 4 and 18; Fig. 1e), one pair of large posterior dorso-lateral pores (LMs 9 and 23; Fig. 1d), and one pair of small posterior dorsal pores (LMs 12 and 26; Fig. 1d). It is unclear whether these seven pores are sensory or excretory organs or both. Regarding sensilla on the cephalothorax, one is medial (LM 30; Fig. 1a–c), while all others are paired; two posterior pairs are located very close to each other (LMs 10 and 11 as well as 24 and 25; Fig. 1d). The outer circular openings of pores and the circular bases of sensilla were used as LMs, and coordinates were taken from the center of each circle. Two specimens that lacked one of the LMs (the most common obvious form of intraspecific variability in harpacticoids) were not used for data collection (arrows are pointing missing LMs 7 and 17 in Fig. 1b and f, respectively). Dorso-lateral cuticular organs on the cephalothorax could also be unquestionably homologized from dorsal view (see Fig. 1a–c), but they were not included in our morphometric analyses because of the potential parallax and distortions related to 2D representation of 3D structures. Two unpaired (medial) LMs (29 and 30) were used to define the longitudinal axis (symmetry axis) on the cephalothorax. Medial LMs were missing on the genital double-somite in *S. akation*, so the longitudinal axis could not be defined and only five LMs were mapped, all on the left side (Fig. 2f). Only one of them was a pore (LM 5), while the other four were all sensilla of similar size; LMs 1 and 2 were always closer to each other than any of them to other LMs. One specimen with a missing LM 4 (arrowed in Fig. 2d) was not used for data acquisition of the genital segment, but was used for data acquisition of the cephalothorax. In total, we sampled LMs from 27 females and 22 males (Table 2). One female (code LN7360f1) was also excluded from our analysis of LMs on the genital double-somite because of the extremely displaced LM 2, even though the same structure on the right side was normally placed (i.e., very close to LM 1).

Morphometric Data Analysis

In order to quantify relative composition of cuticular organs (shape) of both cephalothorax and genital double-somite, we employed 2D landmark-based geometric morphometrics (Bookstein 1991). Pencil drawings of cuticular organs' landmarks were scanned, and 2D Cartesian coordinates from scanned drawings were obtained using tpsDIG 2 software, version 2.17 (Rohlf 2013). Drawings and digitization of landmarks were performed by the same person (T.K.). Cartesian coordinates were aligned using generalized Procrustes superimposition (GPA) (Rohlf and Slice 1990; Dryden and Mardia 1998), which mathematically removes effects of non-shape variation (position, orientation, and scale). During this procedure, size (represented as centroid size) and shape (represented as Procrustes shape coordinates) for each individual were estimated. All procedures related to GPA were done using MorphoJ software (v. 1.06c) (Klingenberg 2011). The cephalothorax is a symmetric structure, and this fact was explicitly taken into account during GPA (Klingenberg et al. 2002). Such adjusted GPA separates shape variation into symmetric and asymmetric components, and only the symmetric component was considered in further analyses. The symmetric component represents "averaging" between left and right sides of the body, where small possible discrepancies induced by positioning specimens relative to the microscope's lens along the transverse axis should be eliminated and thus improve shape estimates.

After extraction of size and shape, a series of exploratory and inferential tests were employed in order to characterize patterns of size and shape variation across clades (A, B, and C) and sexes. Because of the small sample size per group relative to the number of shape variables, inferential tests were based on a non-parametric (np) approach, which uses a residual randomization permutation procedure (RRPP) (Collyer et al. 2015) available in the geomorph package (v. 2.1.3) (Adams and Otárola-Castillo 2013) for R statistical environment (R Core Team 2014). For the same reason, we did not employ ordination methods that rely on inversion of the shape data variance–covariance matrix, such as canonical variate analyses, but rather we used principal component analyses (PCA). In order to characterize patterns of variation attributable to clades and sexes and their interaction we used linear models where statistical evaluation of terms was assessed with RRPP (10,000 iterations). For brevity, depending on the type of response variable(s) used in linear models, we referred to models as npANOVAs when size was

the response variable and npMANOVAs when shape was the response variable. For both approaches, the sum-of-squares (SS) are of type I and the effect of each term in the model was quantified as the amount of variation explained by the term relative to the total variation, and was expressed as coefficient of determination (R^2), ranging from 0 to 1. An effect of size was evaluated with Z score, which is the standard deviation of an effect SS in the random distribution of SS generated by permutations (Collyer et al. 2015). Using Z scores as an effect size will enable one to compare results across studies. It is important to note that SS of terms in the npMANOVAs was assessed using Procrustes distances among specimens, rather than explained covariance matrices among variables. The latter approach is the basis for traditional MANOVA, but it is less effective or even impossible when sample size is small compared with the number of variables. Because clades and sexes showed differences in cephalothorax size (see Results), we analyzed the effect of allometry with the npMANCOVA model where centroid size was used as covariate. Allometry-free (or size corrected) shape data for ordination purposes were obtained as residuals from regression of shape data onto centroid size (Monteiro 1999). PCA was used to characterize and visualize patterns of distribution of individuals in the morphospace defined by the first two PC vectors. Shape changes between consensus shape and mean shape of respective groups were visualized by deformation grids and vector displacements of particular LMs. UPGMA phenograms were constructed based on pairwise Euclidian distances among groups' least squares means. Statistical significance of pairwise distances was evaluated by a permutation test with 10,000 iterations in the geomorph package.

Results

Molecular Phylogeny of Schizopera

Average ML pairwise distances between species were found to be very high (see Supplementary Table S1, available on Dryad at http://dx.doi.org/10.5061/dryad.55q0s), with the lowest divergence (24.6%) between *S. leptafurca* and *S. uranusi*. Divergences between all other taxa were in excess of 25.2%. There was evidence for multiple divergent lineages within the morphospecies *S. akation*, with the average sequence divergence of 14.7% and divergence between haplotypes ranging from 5.3% to 23.1%. All other divergences within morphospecies were below 2.1%.

The ingroup was recovered in all phylogenetic analyses (Fig. 4), and was supported with relatively high bootstrap values (99% for ML and 98% for MP). All our analyses also supported the presence of at least 13 genetically divergent ingroup lineages, corresponding to 13 morphospecies, and all nine of the multisample lineages were supported with high bootstrap values (between 94% and 100%). A sister group relationship between *S. uranusi* and *S. leptafurca* was only relatively weakly supported in our ML analysis, but was moderately supported in our MP analysis. A group comprising *S. uranusi*, *S. leptafurca*, and *S. emphysema* was weakly supported by our PAUP* analyses, but moderately by PhyML; the latter being in accordance with morphological evidence presented in their original descriptions. A relatively well-supported sister group relationship between *S. a. analspinulosa* and *S. analspinulosa linel* was also shown. Relationship among morphologically very similar *S. kronosi* and *S. analspinulosa* was recovered in our ML analyses, but with extremely low bootstrap support. Most basal nodes had very low bootstrap support, which is likely due to saturation at third codon positions, and also to the various lengths of the amplified gene fragments. However, the tree topology did not differ significantly between different methods employed.

The one specimen that did not match our morphospecies (JQ390571.1; preliminary identification as *S.* cf. *uranusi*) formed a separate lineage and is likely to represent an uncharacterized species of *Schizopera*. None of our analyses suggested a particularly close relationship of *S. abei* and *S. akolos*, the only two species in this group with a two-segmented endopod of the fourth leg and previously considered members of a separate genus.

The phylogenetic position of *S. akation* is unresolved, and all our analyses suggested it as a sister clade to all other *Schizopera* species, except for *Schizopera* sp. 2, but the bootstrap support for this relationship was only 21%. However, the structure within this species complex is highly resolved, with high bootstrap values supporting clade A as a sister to two other clades (B+C). This relationship is nicely reflected in their distribution (see Fig. 3), with clade A living furthest downstream in the paleochannel, clade B being collected in the calcrete L, and the most terminal branches of clade C living in the uppermost reaches. This pattern, with intermediate clades living in intermediate calcretes (or bore lines), was also observed in *S. leptafurca* (Fig. 4).

Molecular Species Delimitation

Both ABGD (Fig. 5) and bPTP (Fig. 6 and Supplementary Fig. S2, available on Dryad at http://dx.doi.org/10.5061/dryad.55q0s) single-locus DNA species delimitation methods recovered all three species in the *S. akation* complex. Distribution of pairwise differences in ABGD did not show a clearcut barcode gap (Fig. 5a), but the distribution of differences was more or less bell-shaped. Initial and recursive partitioning in ABGD did not start to diverge until the value of the prior intraspecific divergence fell below 1.29%, which is comparable with some well-studied groups and much larger data sets. This is despite several of our species being represented with less than three sequences, which was shown to be one of the major

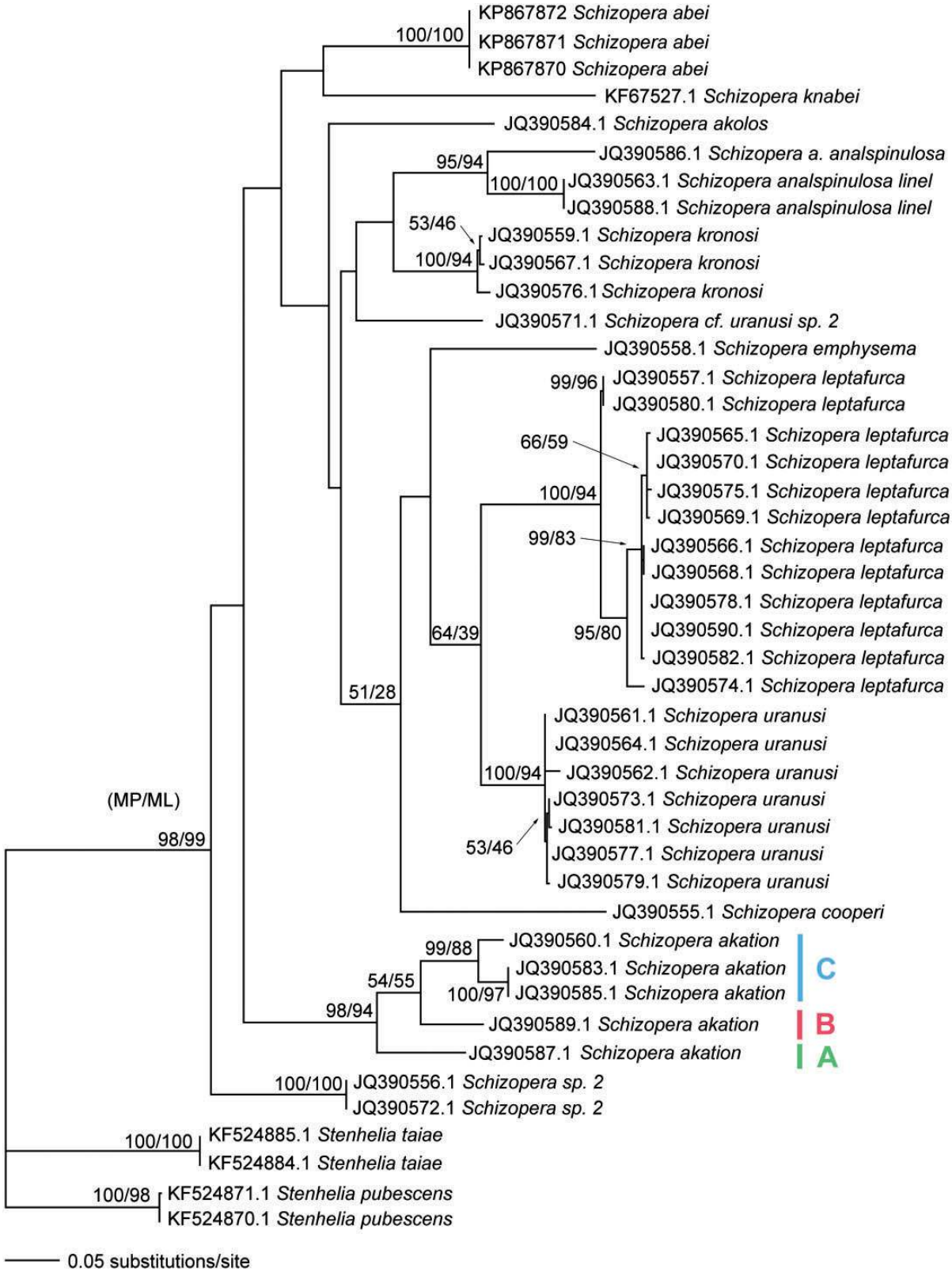

FIGURE 4. Maximum-likelihood tree based on mtCOI sequences of 40 *Schizopera* Sars, 1905 specimens from Australia, Japan, and the USA (see Table 1), constructed using PAUP* 4.0 and an HKY+G+I model of evolution. Numbers on the branches represent bootstrap values above 50% for two different methods (MP/ML) from 1000 pseudoreplicates. The tree is rooted with *Stenhelia taiae* Mu and Huys, 2002 from Korea and *Stenhelia pubescens* Chislenko, 1978 from Russia. The cladogram is drawn to scale and the specimen codes represent their GenBank accession numbers. Three different clades of *Schizopera akation* Karanovic and Cooper, 2012, suggesting three cryptic species are indicated with letters A, B, and C.

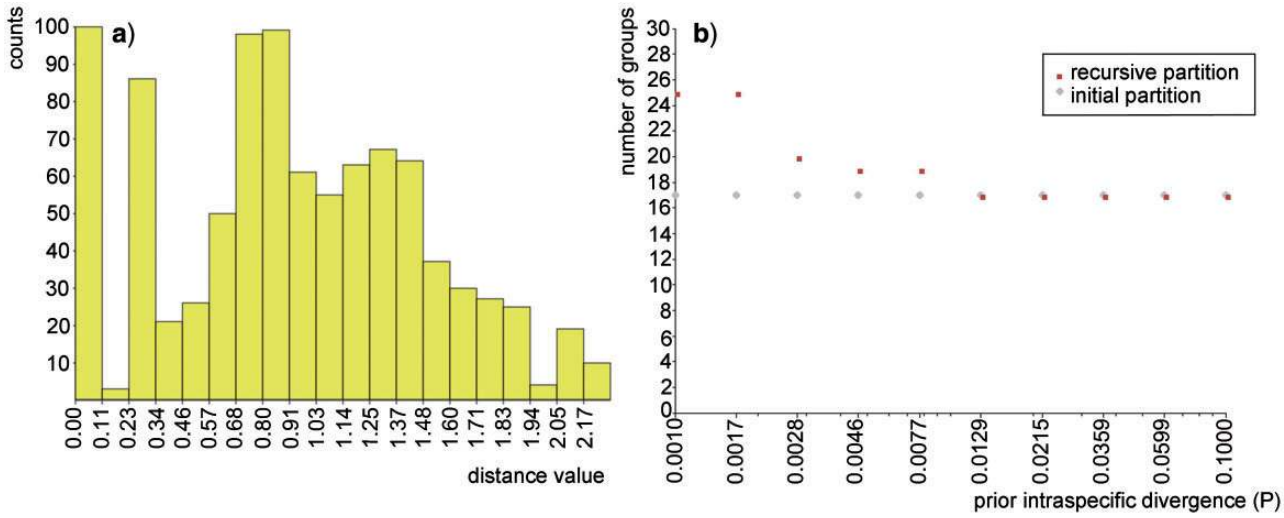

FIGURE 5. Automatic Barcode Gap Discovery (ABGD) outputs, based on ML pairwise distance matrix (HKY+G+I model) as primary input and the value of the proxy for the minimum gap width (*X*) set to 1.1: a) Pairwise distance distribution graph, without a clearcut barcode gap; b) Automatic partition of our data set showing the number of groups inside the partitions (primary and recursive) as a function of the prior limit between intra- and interspecies divergence; note that a prior of 1.3–10% gives the same 17 putative species for both partitions.

weaknesses of this method in simulations (Puillandre et al. 2012). Initial partitioning suggested 17 putative species for all prior values, the only cryptic ones being those in the *S. akation* complex. It recovered the two subspecies of *S. analspinulosa* as distinct species in all cases. Recursive partitioning at prior value of 0.7 suggested three putative groups within *S. leptafurca*, which deserves further biological discussions that are beyond the scope of this article.

Our analyses in bPTP suggested at least 16 putative species (Fig. 6), which is fully congruent with our current level of taxonomy based on morphology. No cryptic species were suggested within *S. leptafurca*, and the two subspecies of *S. analspinulosa* were not separated either. The same three groups are suggested within the *S. akation* complex as in our ABGD analyses, according to geographical isolation of the corresponding populations in different subterranean islands (Fig. 3) and clades (A, B, and C) discovered by morphometric analyses in this study (see below).

Distribution and Homologization of Integumental Organs in Schizopera

All 30 chosen dorsal integumental organs on the cephalothorax (Fig. 1a,c,d,e) and all 5 integumental organs on the left side of the genital double-somite (Fig. 2f) were unquestionably homologized in the *S. akation* complex, based on their nature (pore or sensilla) and/or relative position. Because we had 7 pores and 23 sensilla on the dorsal side of the cephalothorax, the possibility to swap LMs was extremely low, even when some of them had markedly different positions in different lineages. For example, pores LM 12 and LM 26 can be posterior to sensilla LM 11 and LM 25 and nearly as close as sensilla LM 10 and LM 24 (see Fig. 1a) or medial and several lengths further away (see Fig. 1b,c,d), but they can be always homologized without any problems because of their different nature. There was no observable difference between males and females in the number and identity of LMs on the cephalothorax. Homologization is even simpler with four dorsal sensilla and one pore on the genital double-somite, which are all symmetric structures (Fig. 2d,e,f).

Most of the LMs chosen for the morphometric analysis of the cephalothorax in *S. akation* (see below) were present and easily homologized in other examined species of *Schizopera*, but there were also some important differences. For example, all of the other examined species of *Schizopera* lack the rostral pore (LM 29) and the posterior pair of pores (LM 12 and LM 26), and most have one additional pair of pores just posterior to sensilla LM 1 and LM 15 (marked as "x" and "y" in Supplementary Fig. S1, available on Dryad at http://dx.doi.org/10.5061/dryad.55q0s). As in *S. akation*, some specimens were observed with one or two LMs missing on one side, although that was relatively rare, and there was no observable difference between males and females in the number and identity of LMs on the cephalothorax.

The female genital double-somite had only five LMs in *S. akation* (Fig. 2d,e,f) and all of them were present in *S. uranusi* (Fig. 2b), *S. leptafurca* (not shown), and *S. emphysema* (not shown). *Schizopera analspinulosa analspinulosa* (Fig. 2c), *S. analspinulosa linel* (not shown), and *S. kronosi* (not shown) were missing posterior pore LM 5, while *S. cooperi* (Fig. 2a) and *S. abei* (not shown) were missing both the posterior pore LM 5 and the anterior-medial sensilla LM 2. On the other hand, *S. abei* (Fig. 2a) and some specimens of other species were observed with a central anterior pore (not marked on

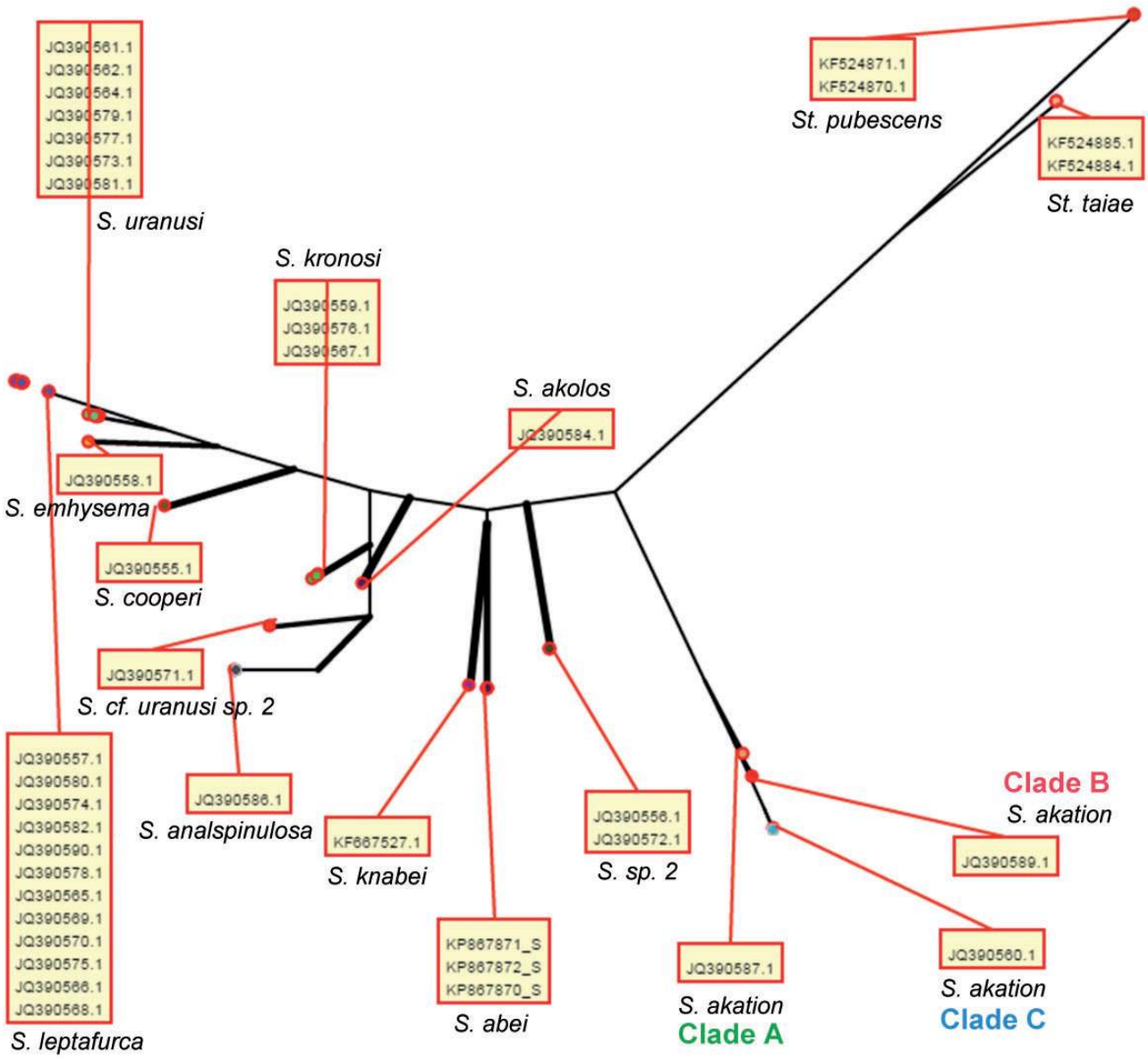

FIGURE 6. PhyloMap visualization of bPTP species delimitation results, with 48.11% of variance explained by the horizontal axis and 16.81% by the vertical axis. A thicker line indicates that the branch length in the original species tree is longer than the branch in the PhyloMap plot. Boxes show only some of GenBank accession numbers for each species (see Fig. 4 and Supplementary Fig. S2, available on Dryad at http://dx.doi.org/10.5061/dryad.55q0s). Three cryptic species in the *Schizopera akation* Karanovic and Cooper, 2012 complex are marked as Clades A, B, and C throughout this article.

any figures), which was very difficult to observe due to its small size and detritus accumulation.

Geometric Morphometrics of the S. akation Complex

Size variation.—Two-factor npANOVA, where response variable was the centroid size of the cephalothorax, showed that both main effects, clade and sex, were highly significant, but their interaction was not (Supplementary Table S2, available on Dryad at http://dx.doi.org/10.5061/dryad.55q0s). Therefore, clades and sexes exhibit size differences, while pattern of sexual size dimorphism is consistent across clades. According to R^2 values, clade effect accounted for 40% of size variation, while sex effect accounted for 18% of size variation after considering the variation explained by clade effect. Clade C individuals appeared to be the largest, followed by clade B individuals, while clade A individuals were the smallest. Surprisingly, the effect of size (Supplementary Table S2, available on Dryad at http://dx.doi.org/10.5061/dryad.55q0s, see Z value) for sex remained higher compared with clade effect (8.4 vs. 7), even when the sex effect entered into the model after the clade term, thus additionally indicating a consistent pattern of sexual size dimorphism (Fig. 7).

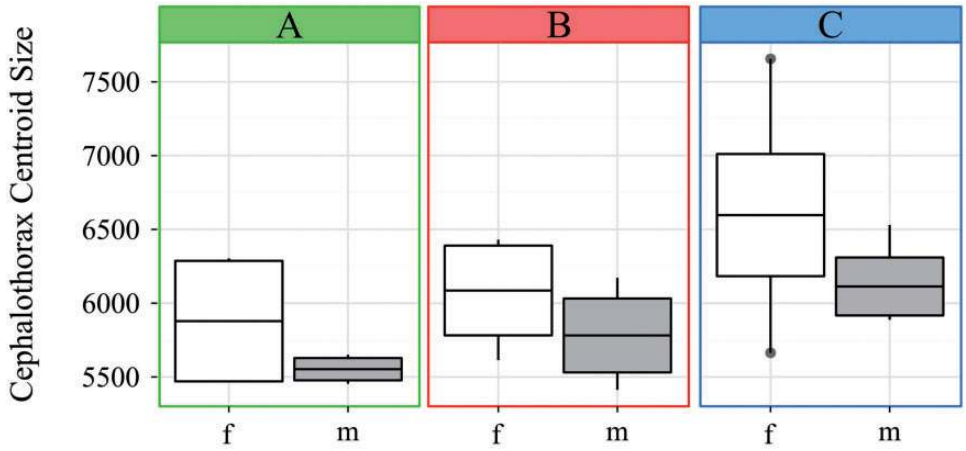

FIGURE 7. Cephalothorax size differences among clades (A–C) and sexes (f and m) of *Schizopera akation* Karanovic and Cooper, 2012. Each box plot is defined by mean value (horizontal mid-box line), span of standard deviation (box), and extreme values (vertical lines).

In contrast to the cephalothorax size variation among clades, one-factor npANOVA where the response variable was centroid size of female's genital double-somite showed that the main effect of clade was not significant (Supplementary Table S3, available on Dryad at http://dx.doi.org/10.5061/dryad.55q0s). There was also a considerable overlap of distributions of size variation among clades (Supplementary Fig. S3, available on Dryad at http://dx.doi.org/10.5061/dryad.55q0s).

Shape variation.—The two-factor npMANOVA where shape data of the cephalothorax were used as response variables indicated that a prominent source of the shape variation was clade factor, accounting for 31% of the overall shape variation (Supplementary Table S4, available on Dryad at http://dx.doi.org/10.5061/dryad.55q0s). Considerably less variation of shape data was explained by the overall sexual shape dimorphism, which was 8%. Furthermore, both main effects were significant. Contrary to this, the interaction term between main effects was not significant, reflecting the fact that the pattern of sexual shape dimorphism was the same across clades. When separate one-way npMANOVAs were performed for clade and sex effects, explained variance remained similar to two-factor npMANOVA (results not shown) additionally justifying the fact that clade affiliation contributed considerably to the overall shape variation.

However, since we detected size differences in the cephalothorax among clades and sexes, we evaluated the influence of allometry on the shape variation with the two-factor npMANCOVA where size was used as covariate (Table 3). In that model, size explained 17% of shape variation suggesting moderate influences of the size-related shape changes to the overall shape variation. Likewise, the clade and sex effects were still significant, but with a bit lower R^2 values compared with the linear model where size was not consider. Allometric lines among groups did not differ significantly, which was indicated by interaction of size covariate and main effects in the model. The pattern of sexual shape dimorphism remained consistent across clades after the size correction (see the interaction of clade and sex).

Shape changes associated with allometry indicated that almost all LMs were equally affected by size differences (Supplementary Fig. S4, available on Dryad at http://dx.doi.org/10.5061/dryad.55q0s). Generally, the cephalothorax appeared slender and shorter in the anterior part and wider and more elongated in the posterior part in larger individuals.

Patterns of the cephalothorax shape variation estimated through npMANOVA and npMANCOVA were consistent with PCA plots (Fig. 8) and UPGMA clusters (Fig. 9). They all showed that variation among clades was more prominent compared with sexual shape dimorphism. The PCA plot of the overall shape variation indicated that the PC1 vector with the load of 26% of the total shape variation separated clade A from clades B and C. The PCA based on the size-corrected shape data showed discrete clustering of the cryptic taxa. The main difference between PCAs based on overall and size-corrected shape data was the shift of the clade C in the morphospace, suggesting that allometry has the strongest impact on that clade. The most distinct feature of clade A compared with the other two clades was the displacement of LMs 12 and 26. Specifically, LMs 12 and 26, respectively, had swapped position in relation to LMs 10, 11 on the left side and 24, 25 on the right side. We were aware of the potential impact of the "Pinocchio effect" (e.g., Von Cramon-Taubadel et al. 2007), where one (paired) LM with considerable variation may distribute its variation to other LMs during the GPA procedure, and thus we performed the same analyses after exclusion of LMs 12 and 26. However, the same patterns of differences were observed with a bit lower statistical support, but still considerably significant (results not shown). The differences between clades C and B were less prominent but they are located in the anterior (LM 4, 16) and

TABLE 3. Shape variation of the cephalothorax inferred by a two-way non-parametric MANCOVA, where size is considered as covariate in the linear model and statistical significance was assessed by a randomized residual permutation procedure (RRPP) with 10,000 permutations

Source	Df[a]	SS[b]	MS[c]	R^{2d}	F^{e}	Z^{f}	P-value[g]
Size	1	138.5E−4	138.5E−4	0.173	12.95	7.43	0.0001
Clade	2	187.1E−4	93.5E−4	0.233	8.75	6.36	0.0001
Sex	1	30.0E−4	30.0E−4	0.037	2.80	2.78	0.0012
Size : Clade	2	9.6E−4	4.8E−4	0.012	0.45	0.49	0.9702
Size : Sex	1	11.0E−4	11.0E−4	0.014	1.03	1.10	0.2580
Clade : Sex	2	19.1E−4	9.5E−4	0.024	0.89	1.03	0.3438
Size : Clade : Sex	2	11.3E−4	5.6E−4	0.014	0.53	0.63	0.8515
Residuals	37	395.7E−4	10.7E−4				
Total	48	802.2E−4					

[a]Degrees of freedom.
[b]Sum of squares.
[c]Mean squares.
[d]Coefficient of determination.
[e]F critical value.
[f]FEffect size measured as standard deviations of observed SS-values from sampling distributions of random values obtained by RRPP.
[g]Probability of finding a random value larger than the observed value.

posterior part (LM 12, 26) of the cephalothorax along the longitudinal axis. For instance, clade B appeared to be more slender and elongated compared with clade C. Contrasts between these clades were more prominent when full shape data were considered because of LMs in the posterior part of the cephalothorax. Overall, clade A was the most distinct compared with clades B and C (see our Supplementary Fig. S5, available on Dryad at http://dx.doi.org/10.5061/dryad.55q0s) and allometry had the strongest impact on clade C.

One-factor npMANOVA where response variables were shape data of the genital double-somite (females only) indicated that the clade term had highly significant and prominent effect, accounting for almost 50% of the total shape variation (Supplementary Table S5, available on Dryad at http://dx.doi.org/10.5061/dryad.55q0s). Allometry did not have any significant contribution to the shape variation, and all subsequent analyses were based on the total shape variation in this data set. Differences among clades based on the shape of the genital double-somite were visualized by PCA (Fig. 10). Clade C clustered in the positive part of the PC1 vector, while clades A and B formed two distinct clusters in the negative part of the PC1 vector. It was notable that most variation was attributable to the relative position of LM 5 (Fig. 10), which was the only pore in the data set, and that most of the variation was found in the posterior half of the genital double-somite, while the anterior part seems to be more conservative. The UPGMA phenogram based on pairwise Euclidean distances among clades suggested that clade C was the most distinct, followed by the cluster formed by clades A and B (Supplementary Fig. S6, available on Dryad at http://dx.doi.org/10.5061/dryad.55q0s).

Taxonomy

Schizopera akation Karanovic and Cooper, 2012 *s. str.*—Synonymy: *Schizopera akation* sp. nov. [partim], Karanovic and Cooper (2012), p. 141, figs. 17, 18, and 21).

Type and only locality: Australia, Western Australia, Yilgarn region, Yeelirrie Station, calcrete SB, line SB (Fig. 3, clade A), bore SB14–1, 27.344283°S 120.307708° E.

Differential diagnosis: Body size generally smaller than in *Schizopera kryphia* sp. nov. or *S. krypta* sp. nov. (Fig. 7). Cephalothorax with pores LM 12 and LM 26 posterior to sensilla LM 11 and LM 25, and nearly as close to each other as sensilla LM 10 and LM 24 (Fig. 1a). Genital double-somite with more than three rows of minute spinules in the posterior half (arrowed in Fig. 2e); dorsal pore LM 5 situated within the anterior band of spinules (Fig. 2e).

Schizopera kryphia sp. nov.—Synonymy: *Schizopera akation* sp. nov. [partim], Karanovic and Cooper (2012, p. 141).

Type locality: Australia, Western Australia, Yilgarn region, Yeelirrie station, calcrete L, line L (Fig. 3, clade B), bore L-UNK1, 27.329832°S 120.150590° E.

Holotype: Female in toto (WAM C55902) on an SEM stub in dorsal view (Fig. 1c).

Differential diagnosis: Body size generally larger than in *S. akation* but smaller than in *S. krypta* sp. nov. (Fig. 7). Cephalothorax with pores LM 12 and LM 26 median to sensilla LM 11 and LM 25, and more than four times further away from them than sensilla LM 10 and LM 24 (Fig. 1c,d). Genital double-somite with three rows of minute spinules in posterior half (Fig. 2f); dorsal pore LM 5 situated between second and third row of spinules in the posterior half (Fig. 2f).

Etymology: The species name comes from the Greek adjective "κρύφιος" (= "kryphios"; meaning "hidden", "secret"), agreeing in gender with the feminine genus name.

Schizopera krypta sp. nov.—Synonymy: *Schizopera akation* sp. nov. [partim], Karanovic and Cooper (2012), p. 141, figs. 19 and 20).

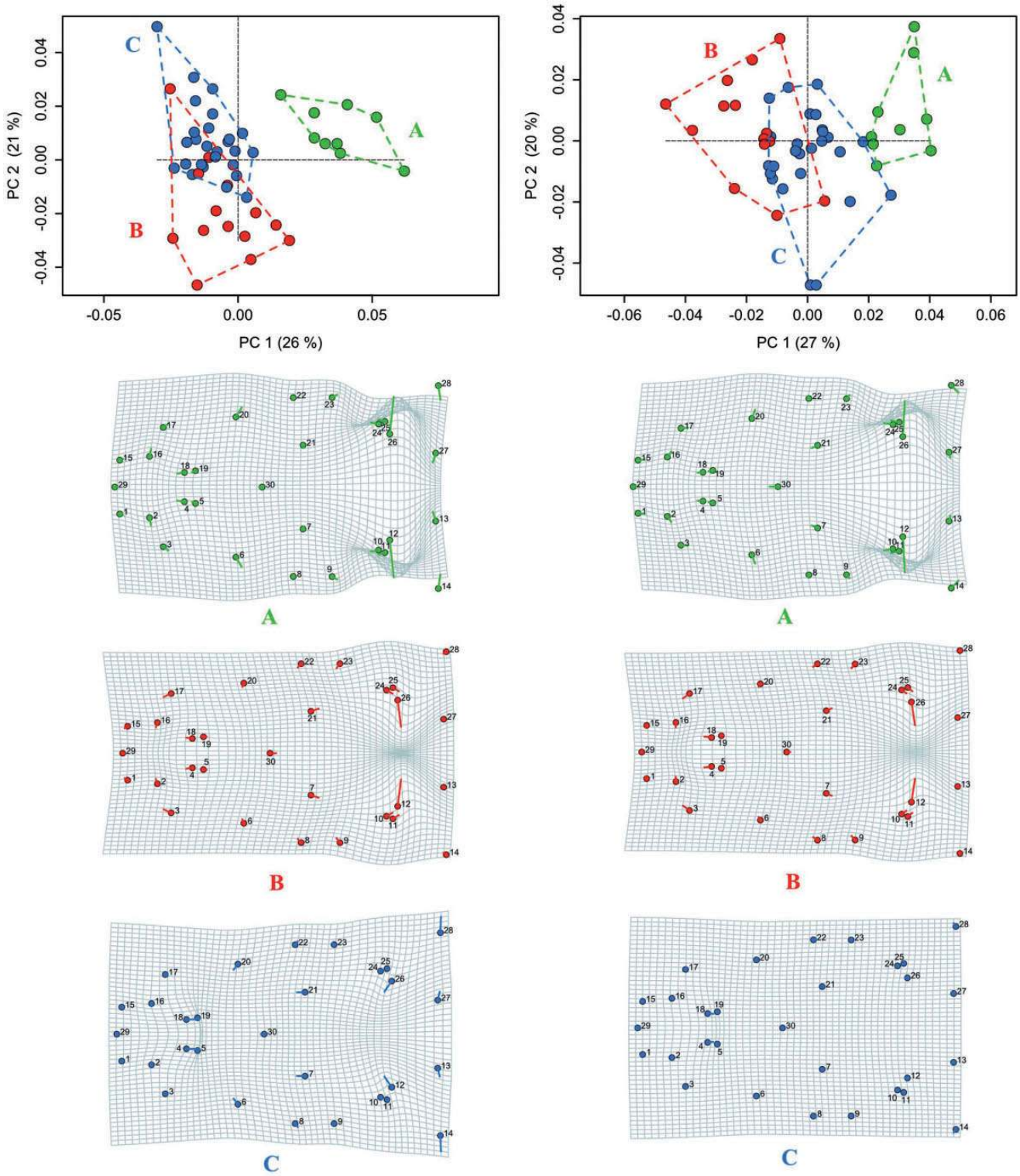

FIGURE 8. Delimitation of *Schizopera akation* Karanovic and Cooper, 2012 clades (A–C) in morphospace and visualization of shape changes of each clade relative to mean shape of the whole sample based on the cephalothorax variation with allometry (left) and without allometry (right). Morphospaces are defined by first two eigenvectors (PCs) of Procrustes coordinates and relative amount of shape variation explained by PCs is provided, along with a convex hull for each group. Transformations grids (scaled 3×) below PC plots visualize shape changes of each clade relative to mean shape of the whole sample.

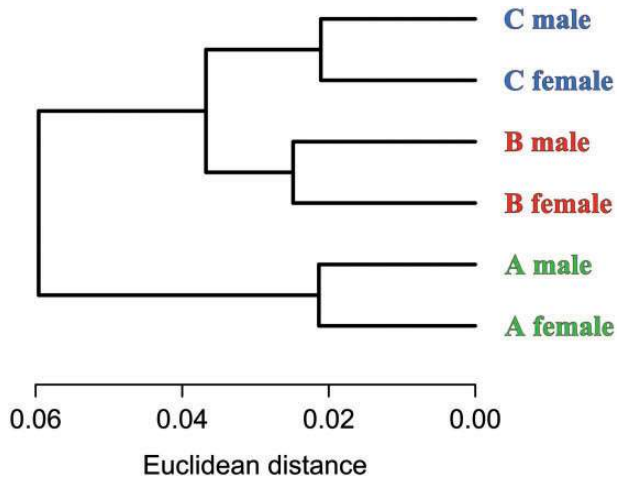

FIGURE 9. UPGMA phenogram based on pairwise Euclidean distances among least square means of clade/sex groups in the cephalothorax data set of *Schizopera akation* Karanovic and Cooper, 2012.

Type locality: Australia, Western Australia, Yilgarn region, Yeelirrie station, calcrete Yeelirrie, line 1 (Fig. 3, clade C), bore YYD22, 27.167304°S 119.870456°E.

Holotype: Female in toto (WAM C55903) on an SEM stub in dorsal view (Fig. 1b).

Differential diagnosis: Body size generally larger than in *S. akation* or *S. kryphia* sp. nov. (Fig. 7). Cephalothorax with pores LM 12 and LM 26 median to sensilla LM 11 and LM 25, and more than four times further away from them than sensilla LM 10 and LM 24 (Fig. 1b). Genital double-somite with three rows of minute spinules in posterior half (Fig. 2d); dorsal pore LM 5 situated between first and second row of spinules in posterior half (Fig. 2d).

Etymology: The species name comes from the Greek adjective "κρυπτός" (= "kryptos"; meaning "hidden"), agreeing in gender with the feminine genus name.

DISCUSSION

Adequate delimitation of species and their formal taxonomic description is one of the prerequisites for the improvement of the conservation process (Mace 2004; Goldstein and DeSalle 2011; Platnick 2013; Pante et al. 2015). In this study we used the pattern of relative distribution of integumental organs in two morphological structures, the cephalothorax and genital double-somite, to delimit cryptic taxa in the *S. akation* complex. The pattern in both structures is in agreement with molecular delimitation analyses that showed the existence of three distinct evolutionary units, clades A, B, and C. Clades B and C are here described as two new species, *S. kryphia* and *S. krypta*, respectively, while clade A was redefined as *S. akation s. str*. In addition to this, our study highlights the following important points: 1) taxonomists should exploit phenotypic features as much as possible, especially rarely used microstructures such as integumental organs; 2) phenotypic features should be analyzed using multivariate tools that explicitly take into account geometry of the phenotype; 3) phenotypic variation analyzed in an explicit geometric context can be as sensitive as molecular data; 4) decrypted species could be formally described using a condensed format that is in agreement with the relevant code; 5) and beyond a direct contribution to taxonomy and systematics, multivariate analyses of phenotypes provide a language that can be further interpreted in evolutionary, ecological, and developmental studies, all of which in turn may help us to understand, explain, characterize, and formalize diversity.

Exploitation of Minute Phenotypic Structures

Since the first comprehensive survey of cuticular organs in copepods by Fleminger (1973), who mapped and coded perforation sites of the dorsal and lateral parts of body tergites in the calanoid genus *Eucalanus* Dana, 1853, these organs have been studied sporadically in several groups of calanoids (Strickler 1975; Mauchline 1977, 1988; Mauchline and Nemoto 1977; Von Vaupel Klein 1982a, 1982b; Malt 1983), cyclopoids (Baribwegure and Dumont 1999; Baribwegure et al. 2001; Baribwegure and Mirabdullayev 2003; Alekseev et al. 2006; Karanovic and Krajicek 2012a; Karanovic et al. 2013a), and harpacticoids (Karanovic et al. 2012, 2013b, 2014; Karanovic and Cho 2012; Karanovic and Lee 2012; Karanovic and McRae 2013; Karanovic and Kim 2014a, 2014b), mostly in the taxonomic context. However, a great majority of taxonomic work on copepods does not extend to the study of these minute structures, and some of the most cited contemporary reference works on copepod morphology either do not mention cuticular organs at all (Huys and Boxshall 1991; Boxshall and Halsey 2004) or refer to them in a single passing sentence (Huys et al. 1996, p. 4). Here we would especially like to advocate their potential use in studies of fossil taxa and old and valuable museum specimens, for which molecular data could not be obtained. Furthermore, their significance for reconstructing phylogenetic relationships among copepods has been recently demonstrated by Karanovic and Kim (2014a), who also postulated that these underutilized microstructures probably evolve under different constraints than do macromorphological structures.

Analyses of Geometric Aspects of the Phenotype

We believe that this study represents the first attempt to utilize pores and sensilla as landmarks for quantification of morphological variation in crustaceans. Cuticular organs were seldom used as landmarks for geometric morphometrics analyses in arthropods in general, with only several recent studies on mites (Baran et al. 2011; Jagersbacher-Baumann and Ebermann 2013; Jagersbacher-Baumann 2014a, 2014b; Shen et al. 2014; Vidović et al. 2014). The relative ease with which cuticular organs can be homologized in closely related

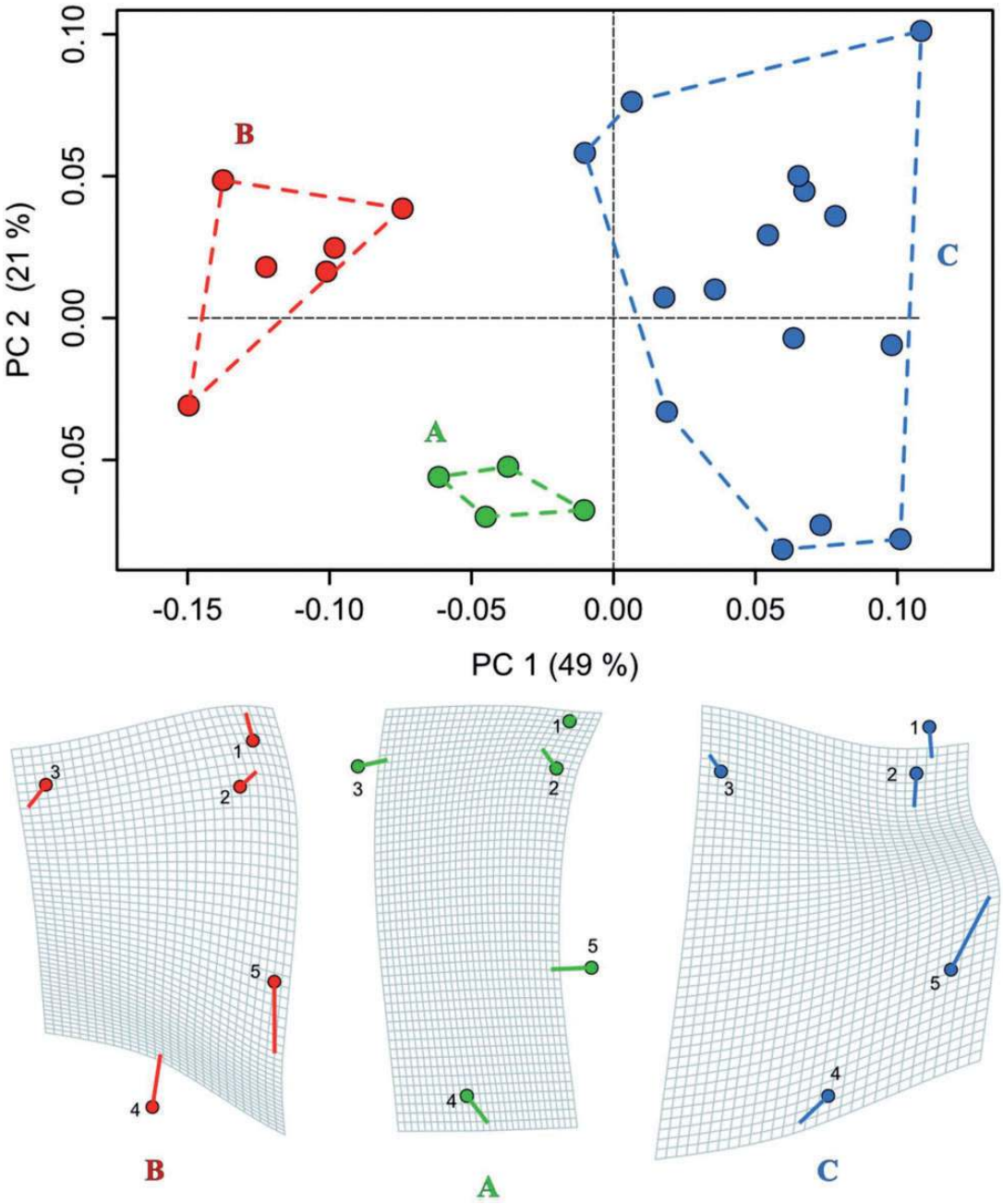

FIGURE 10. Delimitation of *Schizopera akation* Karanovic and Cooper, 2012 clades (A–C) in morphospace and visualization of shape changes of each clade relative to mean shape of the whole sample based on the genital double-somite variation in females. Morphospace is defined by first two eigenvectors (PCs) of Procrustes coordinates and relative amount of shape variation explained by PCs is provided, along with a convex hull for each group. Transformations grids (scaled 3×) below PC plot visualize shape changes of each line relative to mean shape of the whole sample.

taxa (14 species of *Schizopera* analyzed here being a perfect example), and the fact that they represent ideal Type I landmarks for geometric morphometrics (Bookstein 1991), should lead to their much wider use in distinguishing cryptic species. The use of geometric morphometrics as a tool to quantify subtle morphological variation was proven to be fruitful for delimitation of cryptic taxa in various arthropod groups, such as wasps (Baylac et al. 2003; Schwarzfeld and Sperling 2014), hoverflies (Milankov et al. 2009; Francuski et al. 2011), buterflies (Barão et al. 2014), beetles (Andújar et al. 2014; Zúñiga-Reinoso and Benítez 2015), woolly whiteflies (Mottern and Heraty 2014), and some crustaceans (Bracken-Grissom et al. 2011; Marchiori et al. 2014). Congruence between our molecular analyses and geometric morphometrics based on cuticular organs opens new possibilities for the use of these structures and procedures in other crustacean groups, other

arthropods, and most other small animals with a rigid integument, where pervasive practice of taxonomists was to use traditional approaches of analysing mostly qualitative data. As most of our chosen landmarks for *S. akation* were also present in other congeners, there is a possibility for the reconstruction of shape evolution once a more robust phylogenetic tree becomes available.

Multivariate Phenotype and Molecular Data

The widely perceived supremacy of molecular methods in detecting cryptic species (Ladner and Palumbi 2012; Leliaert et al. 2014) is in our view a consequence of disparity in investment between molecular and morphological studies done in the past 20 years (De Carvalho et al. 2007; Stein et al. 2014), and residual typological analysis of phenotypes in classical taxonomy. Our study shows that geometric morphometric analyses of phenotypes can provide as much resolution as molecular data, if not more. For example, using geometric morphometrics we were able to separate sexes of all three cryptic species with high certainty, which is not possible using barcoding alone.

Claims that DNA-based species delimitation may lead to species overestimation or underestimation due to the arbitrary value of the barcode gap (Meier 2008; Puillandre et al. 2012) are valid, but are today mostly resolved with implementation of models that infer putative species boundaries on a given phylogenetic input tree (Zhang et al. 2013). Long synonymy sections for many widely distributed and eurytopic species in most animal groups serve as a reminder that morphology-based taxonomy is no less prone to overestimating diversity, and cryptic species discovered by molecular methods show that the opposite was true in many cases.

Here we do not try to exacerbate the debate regarding the DNA taxonomy versus traditional, morphology-based taxonomy (see Wheeler 2008 and references therein), but rather to emphasize unexploited power of recent advances in morphometrics and their value in taxonomic and systematic practices (MacLeod 2008). Integrative taxonomy (Dayrat 2005), after all, is an approach that evolved to help resolve the taxonomic crisis by employing several lines of evidence (e.g., molecular and morphological data). However, the way in which a phenotype is analyzed may play a key role in potential conflicts between molecular and phenotypic data. A majority of taxonomists still assess morphological structures by looking for eye-visible variations among traits. However, morphological structures are highly complex in regard to both their development and evolutionary history, and describing and relating morphological variation to other hypothetical causes requires full multivariate approaches, where geometric properties of the phenotype are preserved (see Adams et al. 2004, 2013). The power of geometric morphometrics to resolve conflicts in taxonomy is known and the concept of cryptic species is explicitly challenged (e.g., Zúñiga-Reinoso and Benítez 2015). However, geomertic morphometrics is still underexploited in this context, and a preliminary analysis of available literature, where geometric morphometrics was utilized along with molecular data, showed that disagreement between methods is less than 5% (M. Djurakic, unpublished data).

Significance of Formal Description of Species

There are probably thousands of species out there that have been delimited by molecular data alone, but remain without formal description; for a summary on copepods see Lajus et al. (2015). The question is what should we do with them? One solution would be to re-examine them using geometric morphometrics and formally describe them. Journal editors should make such analyses mandatory for all papers, instead of opting to publish molecular analyses and delegating taxonomic descriptions to subsequent contributions and specialized taxonomic journals. In cases where this is not possible due to small sample size, we see no problems in formal species descriptions being based on reliable DNA data alone (see Cook et al. 2010; Stand and Sundberg 2011) or in combination with morphological characters (Harvey et al. 2008; Jörger and Schrödl 2013; Clouse and Wheeler 2014). There is certainly nothing in the Zoological Code (ICZN 1999) to prevent this, provided that other basic criteria (such as holotype designation) are met, and molecular characters are, after all, just characters. Our decrypted species from Yeelirrie are a good example for the urgency of formal descriptions.

Here and elsewhere the term Yeelirrie has been indiscriminately used to describe the existing pastoral station, one of the tributaries of the Carey paleochannel (as Yeelirrie paleochannel), the system of calcrete deposits in this area, and the proposed uranium mine. Yeelirrie is Australia's second-biggest unmined uranium deposit (Needham 2009). Proposed uranium mining in Yeelirrie may involve removal of a significant portion of the largest calcrete deposit, which contains the uranium ore, accompanied by dewatering of the shallow groundwater habitat. This will impact the core stygofauna habitat and may threaten the continued existence of the *S. akation* complex and numerous other locally endemic copepod and other species of stygofauna (Karanovic et al. 2015). Similar cases in other parts of Western Australia strengthen the call for the improvement of conservation procedures in regions where short-range endemics coincide with extraction of mineral resources (Eberhard et al. 2009; Harvey et al. 2011; Karanovic et al. 2013b), and this problem has a global resonance.

Multivariate Phenotype beyond Taxonomy and Systematics

Beside taxonomic utility, geometric morphometric analyses provided preliminary insights into the

differential evolutionary modes for the cephalothorax and genital double-somite in the *S. akation* complex. The three clades showed considerable differences in the cephalothorax size, but not in the genital double-somite size, and the pattern of gradual increases in size of cephalothorax from clades A to C was obvious. Similarly, phenograms of the three clades based on the relative distribution of cuticular organs (shape) of two morphological structures were not congruent. The phenogram based on the shape of cephalothorax is in agreement with molecular data, where B and C form a clade which is a sister to clade A. On the other hand, the phenogram based on variation of the genital double-somite shape suggests that A and B form a clade which is a sister to clade C. Observing contrasting patterns of variation for two morphological structures measured on the same individuals is not a rare phenomenon, especially if the two structures have contrasting functional roles and likely selective regimes (Klingenberg 2010a). The cephalothorax in this group of copepods contains seven pairs of appendages, performing a variety of important survival functions (from feeding to locomotion), while the genital double-somite contains a single pair of reduced appendages, relevant mostly for reproduction (Huys and Boxshall 1991). Furthermore, the gradual pattern of the cephalothorax size variation from clade A to C is in agreement with the pattern of their probable radiation upstream in this paleochannel from marine ancestors (see Karanovic and Cooper 2012; Karanovic et al. 2015; also quite evident in our reconstructed phylogeny of *S. leptafurca*). It is expected that salinity of water decreases upstream, which in turn constrains physiological requirements and possibly overall size in a gradual manner (Litchman et al. 2009).

Even though the proximal causes of size differences are beyond this study, this finding represents a starting direction for further research in this group, and suggests possible environmental impact on the size of cephalothorax but not on the genital double-somite. Even though the overall sample size was not ambiguous, further contrasts between the cephalothorax and genital double-somite are suggestive by comparing distribution of shape variation for the two structures in PCA. Hulls that span the variation of the three clades were partly overlapping in PCA based on the cephalothorax data set, but were clearly separated based on the genital double-somite data. Furthermore, the pattern of shape variation in the genital double-somite data set appeared to be the greatest in clade C compared with the other two groups, which might be a consequence of pooling samples from a broader region. Note that all specimens of clade A were collected in a single bore and are most likely kin, and those belonging to clade B were collected in two neighboring bores, while samples belonging to clade C came from a much wider area and also exhibited divergence of about 4% in the molecular data. Given that the cephalothorax is in agreement with molecular data regarding the topology of clades, and that the genital double-somite reflects a possible divergence within clade C but does not agree with the molecular topology, it is likely that the genital double-somite variation reflects population variation, while the cephalothorax is a more stable trait for a species-level comparison. Because the cephalothorax is a multifunctional morphological structure, it might be expected that stabilizing selection is a dominant source that shapes genetic and developmental processes that give rise to the cephalothorax variation. In that way the cephalothorax variation is constrained in a particular direction (Schluter 1996), and its evolutionary change is preserved over a greater time scale compared with the genital double-somite variation. The allometric relationship between the relative position of integumental organs and the overall cephalothorax size differences across clades additionally corroborated stability of the cephalothorax variation. Static allometric lines of the three clades did not differ, which is expected for closely related species (Klingenberg and Zimmermann 1992; Pélabon et al. 2014; Voje et al. 2014), but see Adams and Nistri (2010). Finally, the consistent pattern of sexual shape dimorphism in size and shape of the cephalothorax additionally supports its conservative nature and possible utility for taxonomical research in copepods.

Supplementary Material

Data available from the Dryad Digital Repository: http://dx.doi.org/10.5061/dryad.55q0s.

Funding

Collecting activities around Lake Biwa were supported by LBM Cooperative Research Project K11-02 and LBM Comprehensive Research Project S11-01 and through the kindness of Dr. Mark Grygier. The work was also partly supported by a grant from the National Institute of Biological Resources (NIBR), funded by the Ministry of Environment of the Republic of Korea [NIBR No. 2015-02-001 to T.K.]. Financial support was provided from the Ministry of Science of Serbia [grant no. 173012 to M.D.] and the Provincial Secretariat for Science and Technological Development, Vojvodina, Serbia (project title: "Molecular and phenotypic diversity of taxa of economic and epidemiological importance, and endangered and endemic species in Europe"). Some specimens studied herein were collected as part of the Yeelirrie Subterranean Fauna Survey 2009–2011 commissioned by BHP Billiton Yeelirrie Development Company Pty Ltd and undertaken by Subterranean Ecology Pty Ltd.

Acknowledgments

We thank Michael Collyer (Western Kentucky University) for useful discussions regarding some morphometric analyses, Guillaume Achaz (Univeristy

of Paris) for the help with the ABGD software, and Frank Anderson (Southern Illinois University) for the help with some PAUP* analyses and many careful edits. We are also very grateful to Kathleen Saint (South Australian Museum) for carrying out some PCR and sequencing analyses. Subterranean Ecology Pty Ltd staff assisted with collection and processing of samples: Giulia Perina, Natalie Krawczyk, Peter Bell, and Shae Callan. The scanning electron microscope was made available through the courtesy of Prof. Jin Hyun Jun (Eulji University, Seoul), and we also want to thank Mr Junho Kim (Eulji University, Seoul) for his technical help. We are very grateful to Dr. Yulia Trebukhova (Institute of Marine Biology, Vladivostok) for collecting the samples of *Stenhelia pubescens* in Russia. We further thank Dr. Kichoon Kim (Hanyang University, Seoul) for collecting the samples of *Stenhellia taiae* in Korea and for his help in the laboratory.

References

Adams D.C., Funk D.J. 1997. Morphometric inferences on sibling species and sexual dimorphism in *Neochlamisus bebbianae* leaf beetles: Multivariate applications of the thin-plate spline. Syst. Biol. 46:180.

Adams D.C., Nistri A. 2010. Ontogenetic convergence and evolution of foot morphology in European cave salamanders (Family: Plethodontidae). BMC Evol. Biol. 10:216.

Adams D.C., Otárola-Castillo E. 2013. geomorph: An r package for the collection and analysis of geometric morphometric shape data. Methods Ecol. Evol. 4:393–399.

Adams D.C., Rohlf F.J., Slice D.E. 2004. Geometric morphometrics: Ten years of progress following the "revolution." Ital. J. Zool. 71:5–16.

Adams D.C., Rohlf F.J., Slice D.E. 2013. A field comes of age: Geometric morphometrics in the 21st century. Hystrix Ital. J. Mamm. 24:7–14.

Alarie Y. 1998. Phylogenetic relationships of Nearctic Colymbetinae (Coleoptera: Adephaga: Dytiscidae) based on chaetotaxic and porotaxic analysis of head capsule and appendages of larvae. Can. Entomol. 130:803–824.

Alekseev V., Dumont H.J., Pensaert J., Baribwegure D., Vanfleteren J.R. 2006. A redescription of *Eucyclops serrulatus* (Fischer, 1851) (Crustacea: Copepoda: Cyclopoida) and some related taxa, with a phylogeny of the *E. serrulatus*-group. Zool. Scr. 35:123–147.

Andújar C., Arribas P., Ruiz C., Serrano J., Gómez-Zurita J. 2014. Integration of conflict into integrative taxonomy: Fitting hybridization in species delimitation of *Mesocarabus* (Coleoptera: Carabidae). Mol. Ecol. 23:4344–4361.

Baran Ş., Altun A., Ayyildiz N., Kence A. 2011. Morphometric analysis of oppiid mites (Acari, Oribatida) collected from Turkey. Exp. Appl. Acarol. 54:411–420.

Barão K.R., Gonçalves G.L., Mielke O.H.H., Kronforst M.R., Moreira G.R.P. 2014. Species boundaries in *Philaethria* butterflies: An integrative taxonomic analysis based on genitalia ultrastructure, wing geometric morphometrics, DNA sequences, and amplified fragment length polymorphisms. Zool. J. Linn. Soc. 170:690–709.

Baribwegure D., Dumont H.J. 1999. The use of integumental pore signature in the characterisation of species of the genus *Thermocyclops* Kiefer, 1927: The case of *Thermocyclops emini* (Mrázek, 1895) (Crustacea: Copepoda: Cyclopoida). Belg. J. Zool. 129:187–200.

Baribwegure D., Mirabdullayev I.M. 2003. *Thermocyclops dumonti* sp. n. (Crustacea, Copepoda), from a temporary waterbody in China. Int. Rev. Hydrobiol. 88:201–211.

Baribwegure D., Thirion C., Dumont H.J. 2001. The integumental pore signature of *Thermocyclops oblongatus* (Sars, 1927) and *T. neglectus* (Sars, 1909), with the description of *Thermocyclops africae* new species, and a comparison with *T. emini* (Mrázek, 1895). Hydrobiologia 458:201–220.

Baylac M., Villemant C., Simbolotti G. 2003. Combining geometric morphometrics with pattern recognition for the investigation of species complexes. Biol. J. Linn. Soc. 80:89–98.

Bickford D., Lohman D.J., Sodhi N.S., Ng P.K.L., Meier R., Winker K., Ingram K.K., Das I. 2007. Cryptic species as a window on diversity and conservation. Trends Ecol. Evol. 22:148–155.

Bláha M., Hulák M., Slouková J., Těšitel J. 2010. Molecular and morphological patterns across *Acanthocyclops vernalis-robustus* species complex (Copepoda, Cyclopoida). Zool. Scr. 39:259–268.

Bookstein F.L. 1991. Morphometric tools for landmark data: Geometry and biology. New York: Cambridge University Press.

Boundrias M.A., Pires J. 2002. Unusual sensory setae of the raptorial *Branchinecta gigas* (Branchiopoda: Anostraca). Hydrobiologia 486:19–27.

Boxshall G.A., Halsey S.H. 2004. An introduction to copepod diversity. UK: The Ray Society.

Bracken-Grissom H.D., Enders T., Jara C.G., Crandall K.A. 2011. Molecular diversity of river versus lake freshwater anomurans in southern Chile (Decapoda: Aeglidae) and morphometric differentiation between species and sexes. In: Held C., Koenemann S., Schubart C.D., editors. Phylogeography and population genetics in crustacea. Boca Raton, FL, USA: CRC Press. p. 313–330.

Bradford T., Adams M., Humphreys W.F., Austin A.D., Cooper S.J.B. 2010. DNA barcoding of stygofauna uncovers cryptic amphipod diversity in a calcrete aquifer in Western Australia's arid zone. Mol. Ecol. Res. 10:41–50.

Burgess R. 2001. An improved protocol for separating meiofauna from sediments using colloidal silica soils. Mar. Ecol. Prog. 214:161–165.

Carstens B.C., Pelletier T.A., Reid N.M., Satler J.D. 2013. How to fail at species delimitation. Mol. Ecol. 22:4369–4383.

Cash-Clark C.E., Martin J.W. 1994. Ultrastructure of the frontal sensory fields in the Lynceidae (Crustacea, Branchiopoda, Laevicaudata). J. Morphol. 221:153–160.

Chessman B., Williams S., Besley C. 2007. Bioassessment of streams with macroinvertebrates: Effect of sampled habitat and taxonomic resolution. J. N. Am. Benthol. Soc. 26:546–565.

Clouse R.M., Wheeler W.C. 2014. Descriptions of two new, cryptic species of Metasiro (Arachnida: Opiliones: Cyphophthalmi: Neogoveidae) from South Carolina, USA, including a discussion of mitochondrial mutation rates. Zootaxa 3814:177–201.

Collyer M., Adams D.C. 2013. Phenotypic trajectory analysis: Comparison of shape change patterns in evolution and ecology. Hystrix Ital. J. Mamm. 24:75–83.

Collyer M.L., Sekora D.J., Adams D.C. 2015. A method for analysis of phenotypic change for phenotypes described by high-dimensional data. Heredity 115:357–365.

Cook L.G., Edwards R.D., Crisp M.D., Hardy N.B. 2010. Need morphology always be required for new species descriptions? Invertebr. Syst. 24:322–326.

Costello M.J., May R.M., Stork N.E. 2013. Can we name Earth's species before they go extinct? Science 339:413–416.

Crouau Y. 1997. Comparison of crustacean and insect mechanoreceptive setae. Int. J. Insect Morphol. Embryol. 26:181–190.

Dayrat B. 2005. Towards integrative taxonomy. Biol. J. Linn. Soc. 85: 407–415.

De Carvalho M.R., Bockmann F.A., Amorim D.S., Brandaõ C.R.F., de Vivo M., de Figueiredo J.L., Britski H.A., de Pinna M.C.C., Menezes N.A., Marques F.P.L., Papavero N., Cancello E.M., Crisci J.V., McEachran J.D., Schelly R.C., Lundberg J.G., Gill A.C., Britz R., Wheeler Q.D., Stiassny M.L.J., Parenti L.R., Page L.M., Wheeler W.C., Faivovich J., Vari R.P., Grande L., Humphries C.J., DeSalle R., Ebach M.C., Nelson G.J. 2007. Taxonomic impediment or impediment to taxonomy? A commentary on systematics and the cybertaxonomic-automation paradigm. Evol. Biol. 34:140–143.

De Carvalho M.R., Ebach M.C., Williams D.M., Nihei S.S., Trefaut Rodrigues M., Grant T., Silveira L.F., Zaher H., Gill A.C., Schelly R.C., Sparks J.S., Bockmann F.A., Séret B., Ho H.C., Grande L., Rieppel O., Dubois A., Ohler A., Faivovich J., Assis L.C.S., Wheeler Q.D., Goldstein P.Z., De Almeida E.A.B., Valdecasas A.G., Nelson G. 2014. Does counting species count as taxonomy? On misrepresenting systematics, yet again. Cladistics 30:322–329.

De Queiroz K. 2007. Species concepts and species delimitation. Syst. Biol. 56:879–886.

D'Haese C.A. 2003. Homology and morphology in Poduromorpha (Hexapoda, Collembola). Eur. J. Entomol. 101:385–407.
Dryden I.L., Mardia K.V. 1998. Statistical shape analysis. Chichester, UK: John Wiley & Sons Ltd.
Easton E.E., Darrow E.M., Spears T., Thistle D. 2014. The mitochondrial genomes of *Amphiascoides atopus* and *Schizopera knabei* (Harpacticoida: Miraciidae) reveal similarities between the copepod orders Harpacticoida and Poecilostomatoida. Gene 538:123–137.
Eberhard S.M., Halse S.A., Williams M.R., Scanlon M.D., Cocking J., Barron H.J. 2009. Exploring the relationship between sampling efficiency and short-range endemism for groundwater fauna in the Pilbara region, Western Australia. Freshw. Biol. 54:885–901.
Elofsson R., Hessler R.R. 1994. Sensory structures associated with the body cuticle of *Hutchinsoniella macracantha* (Cephalocarida). J. Crustac. Biol. 14:454–463.
Faucheux M.J., Kristensen N.P., Yen S.-H. 2006. The antennae of neopseustid moths: Morphology and phylogenetic implications, with special reference to the sensilla (Insecta, Lepidoptera, Neopseustidae). Zool. Anz. 245:131–142.
Finston T.L., Johnson M.S., Humphreys W.F., Eberhard S., Halse S. 2007. Cryptic speciation in two widespread subterranean amphipod genera reflects historical drainage patterns in an ancient landscape. Mol. Ecol. 16:355–365.
Fleminger A. 1973. Pattern, number, variability, and taxonomic significance of integumental organs (sensilla and glandular pores) in the genus *Eucalanus* (Copepoda, Calanoida). Fish. Bull. 71: 965–1010.
Folmer O., Black M., Hoeh W., Lutz R., Vrijenoek R. 1994. DNA primers for amplification of mitochondrial cytochrome c oxidase subunit 1 from diverse metazoan invertebrates. Mol. Mar. Biol. Biotechnol. 3:294–299.
Francuski L., Ludoški J., Vujić A., Milankov V. 2011. Phenotypic evidence for hidden biodiversity in the Merodon aureus group (Diptera, Syrphidae) on the Balkan Peninsula: Conservation implication. J. Insect Conserv. 15:379–388.
Gaston K.J., May R.M. 1992. Taxonomy of taxonomists. Nature 356: 281–282.
Goldstein P.Z., DeSalle R. 2011. Integrating DNA barcode data and taxonomic practice: Determination, discovery, and description. BioEssays 33:135–147.
Guindon S., Gascuel O. 2003. A simple, fast and accurate method to estimate large phylogenies by maximum-likelihood. Syst. Biol. 52:696–704.
Guindon S., Dufayard J.F., Lefort V., Anisimova M., Hordijk W., Gascuel O. 2010. New algorithms and methods to estimate maximum-likelihood phylogenies: Assessing the performance of PhyML 3.0. Syst. Biol. 59:307–321.
Guzik M.T., Austin A.D., Cooper S.J.B., Harvey M.S., Humphreys W.F., Bradford T., Eberhard S.M., King R.A., Leys R., Muirhead K.A., Tomlinson M. 2011. Is the Australian subterranean fauna uniquely diverse? Invertebr. Syst. 24:407–418.
Hallberg E., Hannson B.S. 1999. Arthropod sensilla: Morphology and phylogenetic considerations. Microsc. Res. Tech. 47:428–439.
Hallberg E., Skog M. 2011. Chemosensory sensilla in crustaceans. In: Breitaupt T., Thiel M., editors. Chemical communication in crustaceans. Berlin, Heidelberg: Springer. p.103–121.
Hamrova E., Krajicek M., Karanovic T., Cerny M., Petrusek A. 2012. Congruent patterns of lineage diversity in two species complexes of planktonic crustaceans, *Daphnia longispina* (Cladocera) and *Eucyclops serrulatus* (Copepoda), in East European mountain lakes. Zool. J. Linn. Soc. 166:754–767.
Harvey M.S., Berry O., Edward K.L., Humphreys G. 2008. Molecular and morphological systematics of hypogean schizomids (Schizomida: Hubbardiidae) in semiarid Australia. Invertebr. Syst. 22:167–194.
Harvey M.S., Rix M., Framenau V.W., Hamilton Z., Johnson M.S., Teale R., Humphreys G., Humphreys W.F. 2011. Protecting the innocent: Studying short-range endemic taxa enhances conservation outcomes. Invertebr. Syst. 25:1–10.
Hasegawa M., Kishino H., Yano T. 1985. Dating of the human-ape splitting by a molecular clock of mitochondrial DNA. J. Mol. Evol. 22:160–174.
Hebert P.D.N., Cywinska A., Ball S.L., deWaard J.R. 2003. Biological identifications through DNA barcodes. Proc. R. Soc. Lond. B 270:313–321.
Hebert P.D.N., Stoeckle M.Y., Zemlak T.S., Francis C.M. 2004. Identification of birds through DNA barcodes. PLoS Biol. 2: 1657–1663.
Høeg J.T., Kolbasov G.A. 2002. Lattice organs in y-cyprids of the Facetotecta and their significance in the phylogeny of the Crustacea Thecostraca. Acta Zool. 83:67–79.
Huys R., Boxshall G.A. 1991. Copepod evolution. UK: The Ray Society.
Huys R., Fatih F., Ohtsuka S., Llewellyn-Hughes J. 2012. Evolution of the bomolochiform superfamily complex (Copepoda: Cyclopoida): New insights from ssrDNA and morphology, and origin of umazuracolids from polychaete-infesting ancestors rejected. Int. J. Parasitol. 42:71–92.
Huys R., Gee J.M., Moore C.G., Hamond R. 1996. Marine and brackish water harpacticoid copepods, Part 1 Keys and notes for identification of the species. Synop. Br. Fauna (New Series) 51: 1–348.
Huys R., Llewellyn-Hughes J., Olson P.D., Nagasawa K. 2006. Small subunit rDNA and Bayesian inference reveal *Pectenophilus ornatus* (Copepoda *incertae sedis*) as highly transformed Mytilicolidae, and support assignment of Chondracanthidae and Xarifiidae to Lichomolgoidea (Cyclopoida). Biol. J. Linn. Soc. 87: 403–425.
International Commission on Zoological Nomenclature (ICZN). 1999. International code of zoological nomenclature. 4th ed. UK: The International Trust for Zoological Nomenclature.
Jagersbacher-Baumann J. 2014a. Species differentiation of scutacarid mites (Heterostigmatina) using multivariate morphometric methods. Exp. Appl. Acarol. 62:279–292.
Jagersbacher-Baumann J. 2014b. Traditional and geometric morphometric analyses reveal homogeneity in European *Scutacarus acarorum* Goeze, 1780 populations (Acari: Scutacaridae: Heterostigmatina). J. Nat. Hist. 49:1173–1190.
Jagersbacher-Baumann J., Ebermann E. 2013. Methods for rearing scutacarid mites (Acari, Heterostigmatina) and the influence of laboratory cultures on morphometric variables. Exp. Appl. Acarol. 59:447–462.
Jörger K.M., Schrödl M. 2013. How to describe a cryptic species? Practical challenges of molecular taxonomy. Front. Zool. 10:59.
Karanovic T., Cho J.-L. 2012. Three new ameirid harpacticoids from Korea and first record of *Proameira simplex* (Crustacea: Copepoda: Ameiridae). Zootaxa 3368:91–127.
Karanovic T., Cho J.-L., Lee W. 2012. Redefinition of the parastenocaridid genus *Proserpinicaris* (Copepoda: Harpacticoida), with description of three new species from Korea. J. Nat. Hist. 46:1573–1613.
Karanovic T., Cooper S.J.B. 2011a. Molecular and morphological evidence for short-range endemism in the *Kinnecaris solitaria* complex (Copepoda: Parastenocarididae), with descriptions of seven new species. Zootaxa 3026:1–64.
Karanovic T., Cooper S.J.B. 2011b. Third genus of paratenocaridid copepods from Australia supported by molecular evidence (Copepoda, Harpacticoida). In: Defaye D., Suárez-Morales E., von Vaupel Klein J.C., editors. Crustaceana monographs, studies on freshwater copepoda: A volume in honour of Bernard Dussart. Leiden: Brill. p.293–337.
Karanovic T., Cooper S.J.B. 2012. Explosive radiation of the genus Schizopera on a small subterranean island in Western Australia (Copepoda: Harpacticoida): Unravelling the cases of cryptic speciation, size differentiation and multiple invasions. Invertebr. Syst. 26:115–192.
Karanovic T., Eberhard S.M., Perina G., Callan S. 2013b. Two new subterranean ameirids (Crustacea : Copepoda : Harpacticoida) expose weaknesses in the conservation of short-range endemics threatened by mining developments in Western Australia. Invertebr. Syst. 27:540–566.
Karanovic T., Grygier M., Lee W. 2013a. Endemism of subterranean *Diacyclops* in Korea and Japan, with descriptions of seven new species of the *languidoides*-group and redescriptions of *D. brevifurcus* Ishida, 2006 and *D. suoensis* Itô, 1954 (Crustacea, Copepoda, Cyclopoida). ZooKeys 267:1–76.

Karanovic T., Kim K. 2014a. Suitability of cuticular pores and sensilla for harpacticoid copepod species delineation and phylogenetic reconstruction. Arthropod Struct. Dev. 43:615–658.
Karanovic T., Kim K. 2014b. New insights into polyphyly of the harpacticoid genus *Delavalia* (Crustacea, Copepoda) through morphological and molecular study of an unprecedented diversity of sympatric species in a small South Korean bay. Zootaxa 3783: 1–96.
Karanovic T., Kim K., Grygier M.J. 2015. A new species of *Schizopera* (Copepoda: Harpacticoida) from Japan, its phylogeny based on the mtCOI gene and comments on the genus *Schizoperopsis*. J. Nat. Hist. 49:2493–2526.
Karanovic T., Kim K., Lee W. 2014. Morphological and molecular affinities of two East Asian species of *Stenhelia* (Crustacea, Copepoda, Harpacticoida). ZooKeys 411:105–143.
Karanovic T., Krajicek M. 2012a. When anthropogenic translocation meets cryptic speciation globalised bouillon originates; molecular variability of the cosmopolitan freshwater cyclopoid *Macrocyclops albidus* (Crustacea: Copepoda). Ann. Limnol. Int. J. Lim. 48:63–80.
Karanovic T., Krajicek M. 2012b. First molecular data on the Western Australian *Diacyclops* (Copepoda, Cyclopoida) confirm morphospecies but question size differentiation and monophyly of the *alticola*-group. Crustaceana 85:1549–1569.
Karanovic T., Lee W. 2012. A new species of *Parastenocaris* from Korea, with a re-description of the closely related *P. biwae* from Japan (Copepoda: Harpacticoida: Parastenocarididae). J. Species Res. 1:4–34.
Karanovic T., McRae J. 2013. The genus *Schizopera* (Copepoda, Harpacticoida) in the Pilbara region of Western Australia, with description of a new species and its molecular and morphological affinities. Rec. West. Aust. Mus. 28:119–140.
Keil T. 1997. Functional morphology of insect mechanoreceptors. Microsc. Res. Tech. 39:506–531.
Khalaji-Pirbalouty V. 2014. The morphology, arrangement, and ultrastructure of a new type of microtrich sensilla in marine isopods (Crustacea, Isopoda). Zool. Stud. 53:7.
King R.A., Bradford T., Austin A.D., Humphreys W.F., Cooper S.J.B. 2012. Divergent molecular lineages and not-so-cryptic species: The first descriptions of stygobitic chiltoniid amphipods (Talitroidea: Chiltoniidae) from Western Australia. J. Crustac. Biol. 32:465–488.
Klingenberg C.P. 2010a. Evolution and development of shape: Integrating quantitative approaches. Nat. Rev. Genet. 11:623–635.
Klingenberg C.P. 2011. MorphoJ: An integrated software package for geometric morphometrics. Mol. Ecol. Resour. 11:353–357.
Klingenberg C.P., Barluenga M., Meyer A. 2002. Shape analysis of symmetric structures: Quantifying variation among individuals and asymmetry. Evolution 56:1909–1920.
Klingenberg C.P., McIntyre G.S. 1998. Geometric morphometrics of developmental instability: Analyzing patterns of fluctuating asymmetry with Procrustes methods. Evolution 52:1363–1375.
Klingenberg C.P., Zimmermann M. 1992. Static, ontogenetic, and evolutionary allometry: A multivariate comparison in nine species of water striders. Am. Nat. 140:601–620.
Ladner J.T., Palumbi S.R. 2012. Extensive sympatry, cryptic diversity and introgression throughout the geographic distribution of two coral species complexes. Mol. Ecol. 21:2224–2238.
Lajus D., Sukhikh N., Alekseev V. 2015. Cryptic or pseudocryptic: Can morphological methods inform copepod taxonomy? An analysis of publications and a case study of the *Eurytemora affinis* species complex. Ecol. Evol. 5:2374–2385.
Lee C.E., Remfert J.L., Gelembiuk G.W. 2003. Evolution of physiological tolerance and performance during freshwater invasions. Integr. Comp. Biol. 43:439–449.
Lefébure T., Douady C.J., Gouy M., Gibert J. 2006. Relationship between morphological taxonomy and molecular divergence within Crustacea: Proposal of a molecular threshold to help species delimitation. Mol. Phylogenet. Evol. 40:435–447.
Leliaert F., Verbruggen H., Vanormelingen P., Steen F., López-Bautista J.M., Zuccarello G.C., De Clerck O. 2014. DNA based species delimitation in algae. Eur. J. Phycol. 49:179–196.
Litchman E., Klausmeier C.A., Yoshiyama K. 2009. Contrasting size evolution in marine and freshwater diatoms. Proc. Natl. Acad. Sci. U.S.A. 106:2665–2670.
Mace G.M. 2004. The role of taxonomy in species conservation. Phil. Trans. R. Soc. Lond. B 359:711–719.
MacLeod N. 2008. Understanding morphology in systematic contexts: Three-dimensional specimen ordination and recognition. In: Wheeler Q.D., editor. The new taxonomy. Systematics association special pulication. Vol. 76. Boca Raton (FL): CRC Press. p. 143–210.
Malt S.J. 1983. Polymorphism and pore signature patterns in the copepod genus *Oncaea* Philippi, 1843. J. Mar. Biol. Assoc. U.K. 63:449–466.
Marchiori A.B., Bartholomei-Santos M.L., Santos S. 2014. Intraspecific variation in *Aegla longirostri* (Crustacea: Decapoda: Anomura) revealed by geometric morphometrics: Evidence for ongoing speciation? Biol. J. Linn. Soc. 112:31–39.
Marshall J.C., Arevalo E., Benavides E., Sites J., Sites J.W. Jr. 2006. Delimiting species: Comparing methods for Mendelian characters using lizards of the *Sceloporus grammicus* (Squamata: Phrynosomatidae) complex. Evolution 60:1050–1065.
Mauchline J. 1977. The integumental sensilla and glands of pelagic Crustacea. J. Mar. Biol. Assoc. U.K. 57:973–994.
Mauchline J. 1988. Taxonomic value of pore pattern in the integument of calanoid copepods (Crustacea). J. Zool. 214:697–749.
Mauchline J., Aizawa Y., Ishimary T., Marumo R. 1977. Integumental sensilla of pelagic decapod crustaceans. Mar. Biol. 43:149–155.
Mauchline J., Nemoto T. 1977. The occurrence of integumental organs in copepodid stages of calanoid copepods. Bull. Plankton Soc. Japan 24:108–114.
Meier R. 2008. DNA sequences in taxonomy; opportunities and challenges. In: Wheeler, Q.D., editor. The new taxonomy. Systematics association special pulication. Vol. 76. Boca Raton (FL): CRC Press. p. 95–127.
Meisch C., Wouters K. 2004. Valve surface structure of *Candona neglecta* Sars, 1887 (Crustacea, Ostracoda). Studia Quaternaria 21:15–18.
Meloro C., Cáceres N., Carotenuto F., Sponchiado J., Melo G.L., Passaro F., Raia P. 2014. In and out the Amazonia: Evolutionary ecomorphology in howler and capuchin monkeys. Evol. Biol. 41: 38–51.
Meloro C., Elton S., Louys J., Bishop L.C., Ditchfield P. 2013. Cats in the forest: Predicting habitat adaptations from humerus morphometry in extant and fossil Felidae (Carnivora). Paleobiology 39: 323–344.
Milankov V., Ludoški J., Ståhls G., Stamenković J., Vujić A. 2009. High molecular and phenotypic diversity in the *Merodon avidus* complex (Diptera, Syrphidae): Cryptic speciation in a diverse insect taxon. Zool. J. Linn. Soc. 155:819–833.
Mitrovski-Bogdanović A., Tomanović Ž., Mitrović M., Petrović A., Ivanović A., Žikić V., Starý P., Vorburger C. 2014. The *Praon dorsale-yomenae* s. str. complex (Hymenoptera, Braconidae, Aphidiinae): Species discrimination using geometric morphometrics and molecular markers with description of a new species. Zool. Anz. 253:270–282.
Monteiro L.R. 1999. Multivariate regression models and geometric morphometrics: The search for causal factors in the analysis of shape. Syst. Biol. 48:192–199.
Morrison W.R., Lohr J.L., Duchen P., Wilches R., Trujillo D., Mair M., Renner S.S. 2009. The impact of taxonomic change on conservation: Does it kill, can it save, or is it just irrelevant? Biol. Conserv. 142: 3201–3206.
Mottern J.L., Heraty J.M. 2014. The dead can talk: Museum specimens show the origins of a cryptic species used in biological control. Biol. Control. 71:30–39.
Nebelsick M. 1992. Sensory spots of *Echinoderes capitatus* (Zelinka, 1928) (Kynorhyncha, Cyclorhagida). Acta Zool. 73:185–195.
Needham S. 2009. Yeelirrie uranium deposit in Western Australia. Canberra: Parliament of Australia, Department of Parliamentary Service, Background Note.
Nichols P.B., Nelson D.R., Garey J.R. 2006. A family level analysis of Tardigrade phylogeny. Hydrobiologia 558:53–60.
Oshel P.E., Steele V.J., Steele D.H. 1988. Comparative SEM morphology of amphipod microtrich sensilla. Crustaceana 13(suppl.):100–106.
Olesen J. 1996. External morphology and phylogenetic significance of the dorsal/neck organ in the Conchostraca and the head pores of the cladoceran family Chydoridae (Crustacea, Branchiopoda). Hydrobiologia 330:213–226.

Padial J.M., Miralles A., De la Riva I., Vences M. 2010. The integrative future of taxonomy. Front. Zool. 7:16.
Pante E., Schoelinck C., Puillandre N. 2015. From integrative taxonomy to species description: One step beyond. Syst. Biol. 64:152–160.
Parsons K.J., Albertson R.C. 2013. Unifying and generalizing the two strands of evo-devo. Trends Ecol. Evol. 28:584–591.
Pélabon C., Firmat C., Bolstad G.H., Voje K.L., Houle D., Cassara J., Rouzic A. Le, Hansen T.F. 2014. Evolution of morphological allometry. Ann. N.Y. Acad. Sci. 1320:58–75.
Pfenninger M., Schwenk K. 2007. Cryptic animal species are homogeneously distributed among taxa and biogeographical regions. BMC Evol. Biol. 7:121–127.
Platnick N.I. 2013. The information content of taxon names: A reply to de Queiroz and Donoghue. Syst. Biol. 62:175–176.
Pons J., Barraclough T.G., Gmoez-Zurita J., Cardoso A., Duran D.P., Hazell S., Kamoun S., Sumlin W.D., Vogler A.P. 2006. Sequence-based species delimitation for the DNA taxonomy of undescribed insects. Syst. Biol. 55:595–609.
Posada D., Crandall K.A. 1998. Modeltest: Testing the model of DNA substitution. Bioinformatics 14:817–818.
Powell C.V.L., Halcrow K. 1982. The surface microstructure of marine and terrestrial isopods (Crustacea, Peracarida). Zoomorphologie 101:151–164.
Puillandre N., Lambert A., Brouillet S., Achaz G. 2012. ABGD, Automatic Barcode Gap Discovery for primary species delimitation. Mol. Ecol. 21:1864–1877.
Puri H.S. 1974. Normal pores and the phylogeny of Ostracoda. Geosci. Man 6:137–151.
R Core Team. 2014. R: A language and environment for statistical computing. R Found. Stat. Comput. https://www.r-project.org/.
Rohlf J.F. 2013. tpsDIG 2: Software for digitization of landmarks and outlines, version 2.17, http://life.bio.sunysb.edu/ee/rohlf/software.html.
Rohlf J.F., Slice D.E. 1990. Extensions of the Procustes methods for the optimal superimposition of landmarks. Syst. Zool. 39:40–59.
Sanger T.J., Sherratt E., McGlothlin J.W., Brodie E.D. III, Losos J.B., Abzhanov A. 2013. Convergent evolution of sexula dimorphism in skull shape using distinct developmental strategies. Evolution 67:2180–2193.
Schluter D. 1996. Adaptive radiation along genetic lines of least resistance. Evolution 50:1766–1774.
Schwarzfeld M., Sperling F. 2014. Species delimitation using morphology, morphometrics, and molecules: Definition of the *Ophion scutellaris* Thomson species group, with descriptions of six new species (Hymenoptera, Ichneumonidae). ZooKeys 462:59–114.
Shelton R.G.J., Laverack M.S. 1968. Observations on a redescribed crustacean cuticular sense organ. Comp. Biochem. Phys. 25: 1049–1056.
Shen T.-J., Kuo C.-C., Wang C.-F., Huang K.-W. 2014. Delimitation of a continuous morphological character with unknown prior membership: Application of a finite mixture model to classify scapular setae of *Abacarus panticis*. Exp. Appl. Acarol. 63:361–375.
Sites J.W. Jr, Marshall J.C. 2003. Delimiting species: A Renaissance issue in systematic biology. Trends Ecol. Evol. 18:462–470.
Sørensen M.V., Rho H.S., Min W.-G., Kim D., Chang C.Y. 2012. An exploration of *Echinoderes* (Kinorhyncha: Cyclorhagida) in Korean and neighboring waters, with the description of four new species and a redescription of *E. tchefouensis* Lou, 1934. Zootaxa 3368: 161–196.
Stand M., Sundberg P. 2011. A DNA-based description of a new nemertean (phylum Nemertea) species. Mar. Biol. Res. 7: 63–70.
Stein E.D., Martinez M.C., Stiles S., Miller P.E., Zakharov E.V. 2014. Is DNA barcoding actually cheaper and faster than traditional morphological methods: Results from a survey of freshwater bioassessment efforts in the United States? PLoS One 9:e95525.
Strickler J.R. 1975. Intra- and interspecific information flow among planktonic copepods: Receptors. Int. Ver. Theor. Angew. Limnol. Verh. 19:2951–2958.
Swofford D.L. 2003. PAUP*: Phylogenetic analysis using parsimony (*and other methods). Version 4. Sunderland (MA): Sinauer Associates.
Tamura K., Stecher G., Peterson D., Filipski A., Kumar S. 2013. MEGA6: Molecular evolutionary genetics analysis. Version 6.0. Mol. Biol. Evol. 30:2725–2729.
Tanaka A., Namba T., Tanida K., Takemon Y. 2014. Evaluation of a pump method for unbiased sampling of stream hyporheos. Hydrobiologia 730:29–43.
Thompson J.D., Higgins D.G., Gibson T.J. 1994. CLUSTAL W: Improving the sensitivity of progressive multiple sequence alignment through sequence weighting, position-specific gap penalties and weight matrix choice. Nucleic Acids Res. 22:4673–4680.
Tsukagoshi A. 1990. Ontogenetic change of distributional patterns of pore systems in *Cythere* species and its phylogenetic significance. Lethaia 23:225–241.
Vidović B., Jojić V., Marić I., Marinković S., Hansen R., Petanović R. 2014. Geometric morphometric study of geographic and host-related variability in *Aceria* spp. (Acari: Eriophyoidea) inhabiting *Cirsium* spp. (Asteraceae). Exp. Appl. Acarol. 64:321–335.
Vodă R., Dapporto L., Dincă V., Vila R. 2014. Cryptic matters: Overlooked species generate most butterfly beta-diversity. Ecography 38:405–409.
Voje K.L., Hansen T.F., Egset C.K., Bolstad G.H., Pélabon C. 2014. Allometric constraints and the evolution of allometry. Evolution 68:866–885.
Von Cramon-Taubadel N., Frazier B.C., Lahr M.M. 2007. The problem of assessing landmark error in geometric morphometrics: Theory, methods, and modifications. Am. J. Phys. Anthropol. 134:24–35.
Von Vaupel Klein J.C. 1982a. Structure of integumental perforations in the *Euchirella messinensis* female (Crustacea, Copepoda, Calanoida). Neth. J. Zool. 32:374–394.
Von Vaupel Klein J.C. 1982b. A taxonomic review of the genus *Euchirella* Giesbgrecht, 1999 (Copepoda, Calanoida), II. The type-species, *Euchirella messinensis* (Claus, 1863), A. The female of f. typica. Zool. Verh. 198:1–131.
Wheeler Q.D. 2008. The new taxonomy. Systematics association special pulication. Vol. 76. Boca Raton (FL): CRC Press.
Wiens J.J. 2007. Species delimitation: New approaches for discovering diversity. Syst. Biol. 56:875–878.
Will K.W., Mishler B.D., Wheeler Q.D. 2005. The perils of DNA barcoding and the need for integrative taxonomy. Syst. Biol. 54:844–851.
Winkler G., Dodson J.J., Lee C.E. 2008. Heterogeneity within the native range: Population genetic analyses of sympatric invasive and noninvasive clades of the freshwater invading copepod *Eurytemora affinis*. Mol. Ecol. 17:415–430.
Yu Y., Heinrichs J., Zhu R.L., Schneider H. 2013. Empirical evidence supporting frequent cryptic speciation in epiphyllous liverworts: A case study of the *Cololejeunea lanciloba* complex. PLoS One 8:1–9.
Zhang J., Kapli P., Pavlidis P., Stamatakis A. 2013. A general species delimitation method with applications to phylogenetic placements. Bioinformatics 29:2869–2876.
Zhang J., Mamlouk A.M., Martinetz T., Chang S., Wang J., Hilgenfeld R. 2011. PhyloMap: An algorithm for visualizing relationships of large sequence data sets and its application to the influenza A virus genome. BMC Bioinformatics 12:248.
Zhang Z.Q. 2011. Animal biodiversity: An introduction to higher-level classification and taxonomic richness. Zootaxa 3148:7–12.
Zimmer A., Araujo P.B., Bond-Buckup G. 2009. Diversity and arrangement of the cuticular structures of *Hyalella* (Crustacea: Amphipoda: Dogielinotidae) and their use in taxonomy. Zoologia 26:127–142.
Zúñiga-Reinoso Á., Benítez H.A. 2015. The overrated use of the morphological cryptic species concept: An example with *Nyctelia* darkbeetles (Coleoptera: Tenebrionidae) using geometric morphometrics. Zool. Anz. 255:47–53.